Available online at www.sciencedirect.com

ScienceDirect

Journal of Asian Earth Sciences 29 (2007) 1–17

Journal of Asian Earth Sciences

www.elsevier.com/locate/jaes

# Crustal contamination of Late Neogene basalts in the Dien Bien Phu Basin, NW Vietnam: Some insights from petrological and geochronological studies

Ewa Koszowska [a], Anna Wolska [a], Witold Zuchiewicz [a,*], Nguyen Quoc Cuong [b], Zoltan Pécskay [c]

[a] *Institute of Geological Sciences, Jagiellonian University, Oleandry 2A, PL-30063 Kraków, Poland*
[b] *Institute of Geological Sciences, Polish Academy of Sciences, Research Centre in Kraków, Senacka 1, PL-31002 Kraków, Poland*
[c] *Institute of Nuclear Research of the Hungarian Academy of Sciences, 4001 Debrecen, Bem tér 18/C, Hungary*

Received 8 November 2004; accepted 18 December 2005

**Abstract**

Early Pliocene (Zanclean) basalts in the Dien Bien Phu pull-apart basin in NW Vietnam, associated with the presently sinistral Dien Bien Phu Fault Zone, have been dated by the K–Ar method at 4.4–4.9 and 5.4–5.2 Ma. Rapid migration of basaltic magma to the surface in the Dien Bien Phu Fault Zone may be due to Pliocene transtension of the crust in this region, resulting from asthenospheric upwelling induced by lateral displacement of the mantle. The basalts are moderately phyric ( < 10%) and consist of olivine (hyalosiderite), plagioclase (bytownite–labradorite) and orthopyroxene (bytownite–labradorite) phenocrysts, and a fine-grained crystalline matrix (olivine–hortonolite, plagioclase–labradorite, clinopyroxene–pigeonite and augite, K-feldspar). The presence of Fe-rich olivine and orthopyroxene phenocrysts indicates that the basalts are $SiO_2$-saturated/oversaturated olivine tholeiites which formed under water-undersaturated conditions. The Dien Bien Phu basalts contain both mantle-derived (pyroxenites, dunites, gabbros) and crustal (sillimanite/mullite + Mg–Fe spinel), wallrock xenoliths, indicative of crustal contamination during the ascent of the basaltic magma. The basalts show selective enrichment in some mobile elements (K, Rb, Sr and Th), a feature considered to be a result of metasomatism. These rocks, classified on the basis of their normative composition as quartz tholeiites, could represent primary olivine tholeiites/basalts, in which the geochemical signatures were modified by the processes of contamination.


*Keywords:* Petrology; Geochronology; Within-plate basalts; Late Tertiary; Dien Bien Phu Fault Zone

## 1. Introduction

Recently collected samples of Late Neogene basalts associated with the Dien Bien Phu Fault Zone (DBPFZ) in NW Vietnam were examined to constrain the age of Late Cenozoic eruptions in this area and characterise the nature and origin of young within-plate volcanics.

Unlike basalts derived from other regions of SE Asia, the samples from the Dien Bien Phu area are considered to be a product of a single magmatic episode. They display some petrographic and, particularly, some geochemical features that differ from those of other Vietnamese basalts (Hoang et al., 1996a,b; Hoang and Flower, 1998). Therefore, these samples have been examined in detail.

Cenozoic basalts in Vietnam penetrate distinct structural units that are underlain by Precambrian, Palaeozoic and Mesozoic crust in variable proportions (Hutchison, 1989; Tung and Tri, 1992). Significant plate-boundary reorganization in this portion of SE Asia occurred at 45, 25 and 5 Ma; the second event being the most important (Hall, 2002). Cenozoic magmatism in this area is considered to reflect mid-Miocene relocation of lithospheric extension after the cessation of opening of the South China Sea, at about

* Corresponding author. Tel./fax: +48 12 6332270.
*E-mail address:* witold@ing.uj.edu.pl (W. Zuchiewicz).

1367-9120/$ - see front matter © 2006 Elsevier Ltd. All rights reserved.
doi:10.1016/j.jseaes.2005.12.003

16 Ma (Le Pichon et al., 1992; Hoang and Flower, 1998). The proto-South China Sea opened in the Palaeogene (65–34 Ma), whereas the NE part of the South China Sea originated in the Neogene, mostly between 12 and 3 Ma (Zhu et al., 2004). This opening resulted either from extrusion of the Indochina lithosphere due to collision between India and Eurasia (Tapponnier et al., 1986; Briais et al., 1993), or represents Pacific plate-induced back-arc spreading (Taylor and Hayes, 1983). According to Flower et al. (1998), collision-induced extrusion of the asthenospheric mantle was the driving force of both lithosphere escape and marginal basin opening, providing as well the thermal energy required for extension-related basalt magmatism (cf. also Flower and Coban, 2002; Flower et al., 2004).

Basaltic plateaus are found in southern and central Vietnam, while scattered eruptive centres prevail in northern Vietnam (Fig. 1). The majority of these centres are associated with pull-apart basins (Rangin et al., 1995). Hoang et al. (1996a,b) and Hoang and Flower (1998) recognised two eruptive episodes: an early episode (16–9 Ma) producing quartz and olivine tholeiites, with rare alkali basalts, and a later episode (post-dating 8 Ma) erupting olivine tholeiites, alkali basalts, and from the late Pliocene onwards, basanite and rare nephelinite. The two episodes (tholeiites–alkali basalts) were recognised at each large eruptive centre, associated, respectively, with eruptions from extensional fissures, and central eruptions sited on conjugate strike-slip faults.

In northern Vietnam, Cenozoic eruptions occurred at Dien Bien Phu, Phu Quy, Con Co island and Khe Sanh (Hoang et al., 1996a; Hoang and Flower, 1998). The petrology and geochemistry of the eruptions in the Dien Bien Phu area in the northwesternmost part of this zone (Figs. 1 and 2), have so far received little attention.

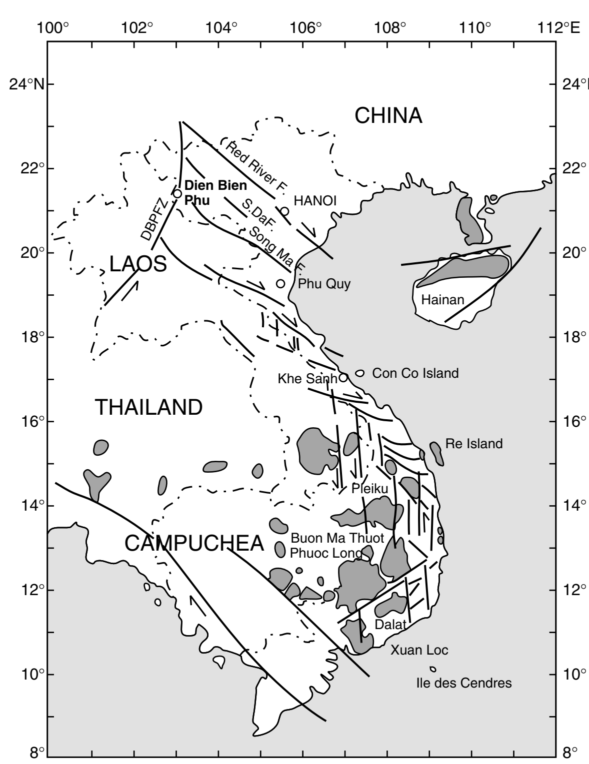


Fig. 1. Cenozoic basaltic volcanic centres in SE Asia (based on Hoang et al., 1996a; Cung et al., 1998; Lepvrier et al., 2004; simplified).

## 2. Study area

The Dien Bien Phu Fault Zone (DBPFZ), orientated NNE-SSW to N–S, is one of the most seismically active fault zones in Indochina. In NW Vietnam, it extends for 160 km and is 6–10 km wide (Figs. 2 and 3), cutting sedimentary and metamorphic rocks of Late Proterozoic, Palaeozoic and Mesozoic age, and Palaeozoic and Upper Triassic granitoids (Figs. 2 and 4).

In contrast to the recently dextral Red River (Song Hong) Fault Zone (RRFZ), the DBPFZ is a sinistral, probably conjugate, fault (cf. Zuchiewicz et al., 2004). The structural evolution of the RRFZ has been interpreted extensively by numerous authors (cf. Tapponnier et al., 1990; Leloup et al., 1995; Cuong and Zuchiewicz, 2001; and references therein), whereas the pre-Quaternary development of DBPFZ still requires reconstruction.

The RRFZ marks the boundary between the South China and Indochina blocks, which is believed to have evolved in two phases: (1) an episode of sinistral ductile shear active between 27 and 16 Ma; followed by (2) a period of exhumation and uplift from depths of 20–25 km, accompanied by dextral, predominantly brittle shear, active during the Plio-Quaternary (Leloup et al., 1995; and references therein). According to Jolivet et al. (2001), the RRFZ is rooted in a horizontal shear zone at the brittle/ductile transition separating the upper and middle crust from the lower crust, sinistral strike-slip motion having been first transpressional (?40–25 Ma), and then transtensional, leading to fast exhumation from 24 to 17 Ma. Wang et al. (1998a,b) maintain that sinistral shearing took place between 27 and 17 Ma. However, recent fission-track studies indicate that the main period of ductile deformation in the RRFZ had terminated by 25 Ma (Anczkiewicz et al., 2000) or 26 Ma (Zelazniewicz et al., 2005). New structural and geochronological data appear to document a polyphase ductile shear active between Early Cretaceous through to Miocene times, which included dextral, sinistral, dextral transpressional, and sinistral transtensional regimes (Zelazniewicz et al., 2005). The Late Miocene change in the sense of motion is commonly attributed to the collision between India and Eurasia (Tapponnier et al., 1990; Schaerer et al., 1994; Harrison et al., 1995). The pre-Pliocene history of the DBPFZ is poorly constrained, although its recent sinistral motion is now firmly established (Wang et al., 1998a,b; Hung and Vinh, 2001; Zuchiewicz and Cuong, 2002; Zuchiewicz et al., 2004).

## 3. Geological setting

In central and northern Vietnam, the Truong Son Belt and the Kontum Massif compose the Indochina (Sunda-

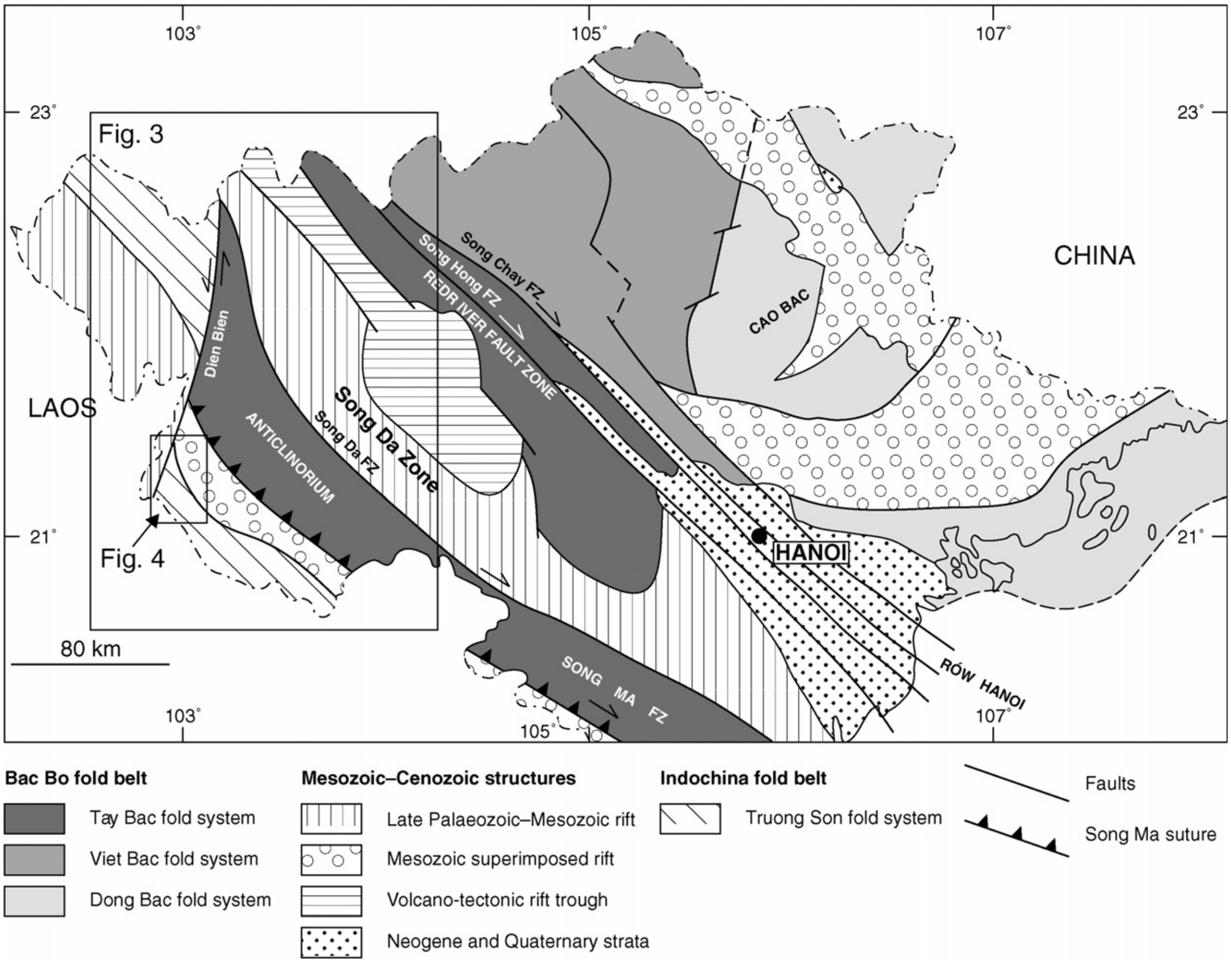


Fig. 2. Simplified geological map of Northern Vietnam (based on Tri, 1979; modified).

land) Block, whereas the NE part of Vietnam belongs to the South China Block (Tri, 1979; Tapponnier et al., 1990; Fontaine and Workman, 1997; Lepvrier et al., 2004).

The Dien Bien Phu Fault Zone (DBPFZ) cuts sedimentary and metamorphic rocks of Late Proterozoic, Palaeozoic and Mesozoic age, as well as granitoid intrusions of the Dien Bien Phu (Palaeozoic) and Kim Bai (Upper Triassic) complexes (cf. My et al., 1978; Tuyet et al., 1978) in the northern part of the Truong Son Belt (Tri, 1979; Fontaine and Workman, 1997), northwestern Vietnam. The DBPFZ is the northern continuation of the Bentong–Raub and Nan Uttaradit (or Uttaradit–Luang Prabang) sutures of Peninsular Malaysia and Thailand (Hutchison, 1975; Maluski et al., 2002). To the southeast of this zone, Silurian–Devonian flyschoid shales and acid volcanic tuffs intruded by granitoids and granites are exposed, followed farther north by ultramafic and mafic rocks representing a disrupted ophiolitic belt within the Song Ma Suture (Fig. 2), thrust on to Palaeozoic strata (Hutchison, 1975; Lepvrier et al., 2004).

The Song Ma Suture formed the boundary between the South China and Indochina blocks during the Indosinian (Early Triassic) orogeny (Maluski et al., 2001, 2002). The West Bac Bo Fold System extends between the Song Ma Suture and the Chay River Fault (Tri, 1979; Yem et al., 2002; cf. Fig. 2). To the north of the Song Ma Suture, a deformed Upper Proterozoic and Lower Palaeozoic metamorphic belt occurs as a broad antiform, called the Song Ma Anticlinorium (Tri, 1979; Yem et al., 2002). Farther north, mafic and ultramafic rocks intercalated in a Permian–Early Triassic terrigeneous-carbonate sedimentary succession form the strongly folded Song Da zone, which is unconformably overlain by Cretaceous red beds (Leloup et al., 1995; Lepvrier et al., 2004; cf. Figs. 2 and 4). This zone has been interpreted as either a continental rift, composed of Late Permian picrite–basalt complexes and an Early Triassic komatiite–basalt association (Tri, 1979; Hutchison, 1989; Polyakov et al., 2002), or the ophiolitic remnants of an ocean basin that closed in the Late Triassic (Hutchison, 1989; Maluski et al., 2001; Lepvrier et al., 2004). The Song Da zone is bounded to the south by the Song Da Fault (Fig. 2), which developed during the pre-Norian Indosinian phase, and a post-Cretaceous shortening event (Lacassin et al., 1998) associated with NE-thrusting, combined with sinistral strike-slip movement on the NW–SE fault (Lepvrier et al., 2004).

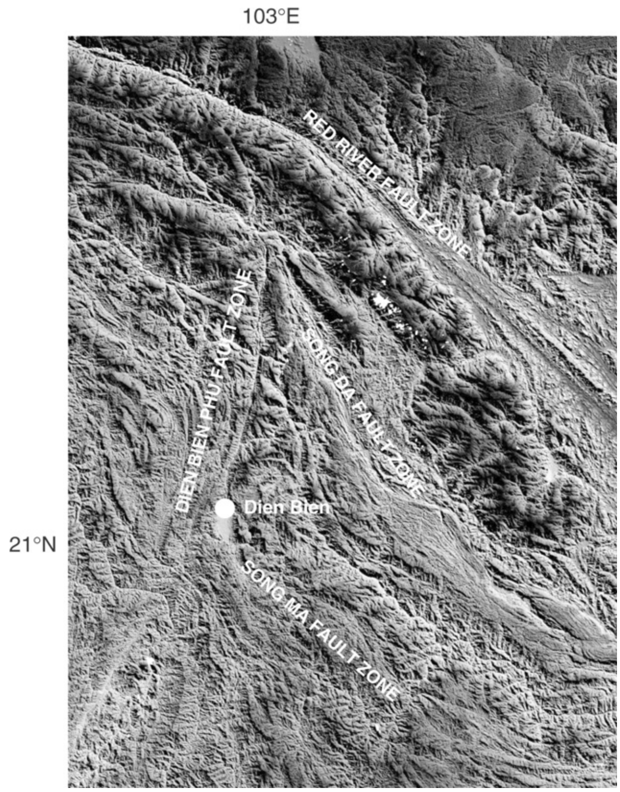


Fig. 3. Satellite radar (SAR) image of principal fault zones in NW Vietnam, based on 30-second GTOPO 30 grid data provided by USGS.

The main fault and the associated subsidiary faults of the DBPFZ are strike-slip and oblique in character. The principal fault plane dips 60–70° to the west in the northern part and 70–80° (even 90°) in the southern part of the zone (Hung and Vinh, 2001). Mesozoic exposures are dextrally offset by 45–50 km, although the fault is presently sinistral and normal-sinistral, the normal component increasing to the north (Tapponnier et al., 1986; Wang et al., 1998a,b; Hung and Vinh, 2001; Zuchiewicz et al., 2004). Dextral faulting was completed either in the Early Cretaceous (Leloup et al., 1995; Wemmer et al., 1999) or Late Miocene (Kiem et al., 1999; Trinh et al., 1999; Hung and Vinh, 2001). The amount of recent sinistral offset has been estimated at 250–800 m (Trinh et al., 1993) to > 2 km (Hung and Vinh, 2001), although Zuchiewicz et al. (2004) document offsets ranging from 6–8 to 150 m for the Holocene to 1.2–9.75 km for middle through late Pleistocene time.

The fault zone is accompanied by a few narrow pull-apart basins, the southernmost and largest of which is the Dien Bien Phu Basin (Figs. 3 and 4). Immediately north of the basin, the fault zone is accompanied by exposures of Upper Neogene tholeiitic basalts (Hoang et al., 1996a,b; Lee et al., 1998), thermal springs, and emanations of radon, methane and carbon dioxide (Hung and Vinh, 2001), and is marked by epicentres of relatively strong earthquakes. Young basalts have been drilled in the basin bottom, some 2 km west of Dien Bien city (borehole LK-3D; cf. Figs. 4 and 5). These lie beneath a 130 m-thick series of Pliocene (?)-Quaternary terrestrial sediments (Dy et al., 1999; Zuchiewicz et al., 2004), and are hosted by Upper Triassic (Norian–Rhaetian) siltstones and claystones.

## 4. Sampling and petrography

### *4.1. Sampling*

Several samples of the basalts and their thermally altered wallrocks were examined using petrographic and geochemical methods. The basalts were collected from surficial exposures (DB 54, VA 24) located north of Dien Bien (Fig. 4), and from borehole LK-3D (at a depth of 130 m) situated a short distance west of Dien Bien (Figs. 4 and 5), while thermally altered wallrocks (DB 52a, DB 52/1) were sampled from the above-mentioned surficial exposures.

The wallrocks are very hard, black or dark green metapelites (samples: DB 52a, DB 52/1). These very fine-grained rocks consist of angular detrital quartz, detrital white mica, neogenic chlorite (clinochlore) and pyrite. The wallrocks were weakly altered under conditions of lower-grade thermal metamorphism, probably corresponding to the lower range of the albite–epidote–hornfels facies.

### *4.2. Petrography*

Petrographic study of samples DB 54, VA 24, and LK-3D was performed using AMPLIVAL petrographic optical microscope. Macroscopically, the basalts appear black and aphyric. Microscopic observations indicate that the structure is fine-grained and porphyritic, whilst the texture is generally chaotic, but aligned locally, due to the parallel orientation of plagioclase laths.

The basalts contain small mafic and ultramafic plutonic enclaves (1.3–2.4, and 1.7–3.3 mm in size) (gabbros, pyroxenites, and dunites), showing cumulate textures. Gabbros consist of plagioclases $Ab_{36–47}An_{68–50}Or_{3–2}$ (labradorite), orthopyroxenes $En_{75–62}Wo_{5–4}Fs_{33–21}$ (bronzite–hypersthene), and two variants of clinopyroxene: $En_{55–45}Wo_{8–16}Fs_{37–39}$ (pigeonites) and $En_{45}Wo_{20}Fs_{33}$ (augites). Pyroxenites contain: orthopyroxenes $En_{79–57}Wo_{3–5}Fs_{18–38}$ (bronzite–hypersthene), clinopyroxenes $En_{59}Wo_{6}Fs_{35}$ (pigeonites) and $En_{44–41}Wo_{41–36}Fs_{18–20}$ (augites), whereas dunites consist of olivine $Fo_{81–79}$ (chrysolite).

In the basalt groundmass, twinned labradoritic plagioclase ($An_{66–51}$ with 3–5 mol% Or) laths, xenomorphic crystals of clinopyroxene (pigeonite $Wo_{16–6}En_{55–42}Fs_{53–35}$, augite $Wo_{42–30}En_{42–30}Fs_{32–25}$) and olivine ($Fo_{48–37}$) are observed. Most crystals in the groundmass are 0.01–0.2 mm in size. In the interstices between the plagioclase laths, clinopyroxene and olivine xenomorphic crystals of potassium-feldspar ($Or_{79–60}$ with 3 mol% An) are observed. More abundant xenomorphic crystals of K-feldspars occur in the groundmass of sample LK-3D, while dispersed opaque mineral grains (Fe–Ti oxides) and rare pentlandite (Fe–Ni sulphides) is also observed.

Plagioclase, olivine and pyroxene phenocrysts are distinctly larger, and chaotically distributed in the ground-

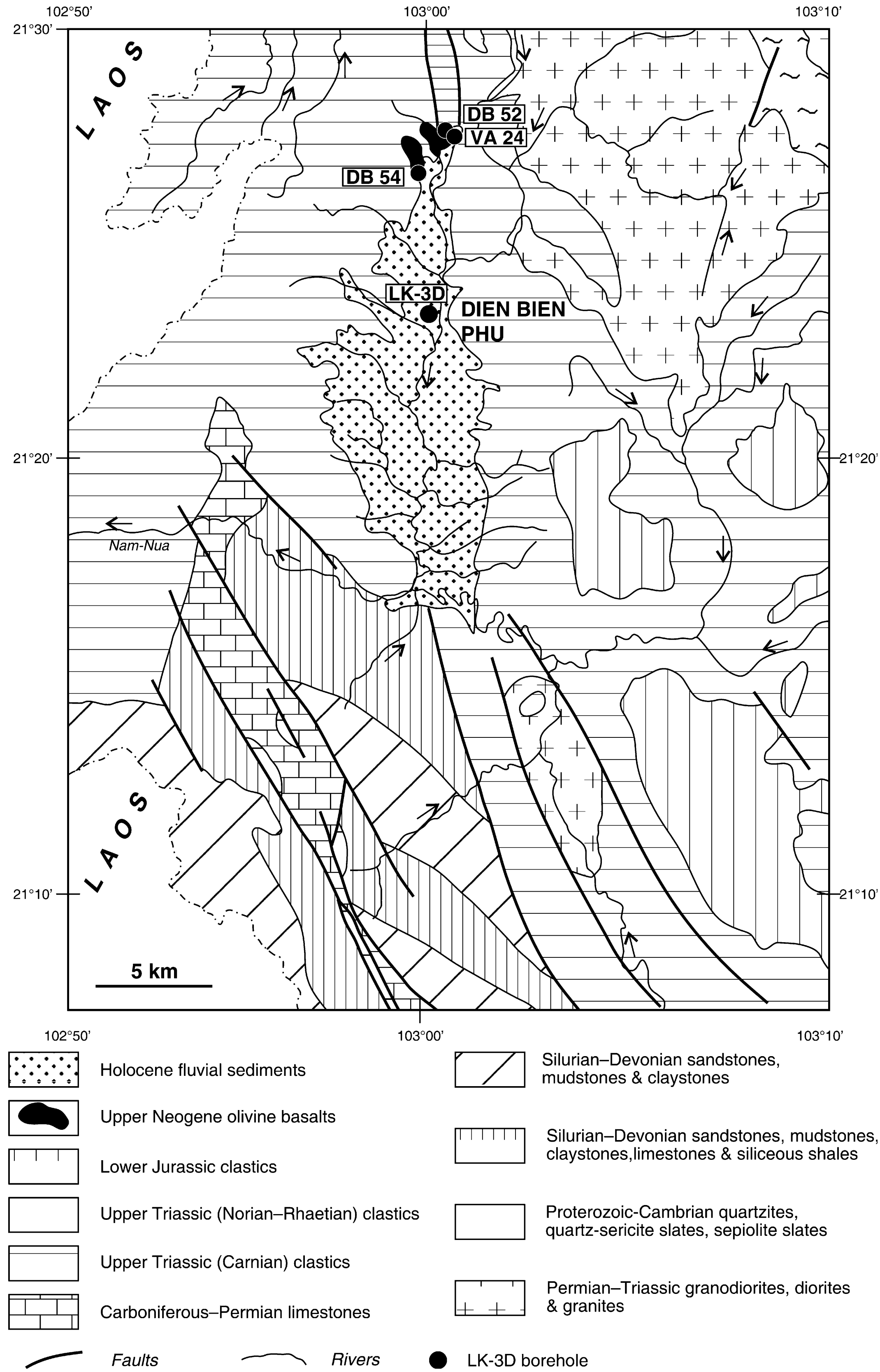


Fig. 4. Simplified geological map of the Dien Bien Phu area, showing sampling sites (based on My et al., 1978; Tuyet et al., 1978; Son, 1978; see also Zuchiewicz et al., 2004).

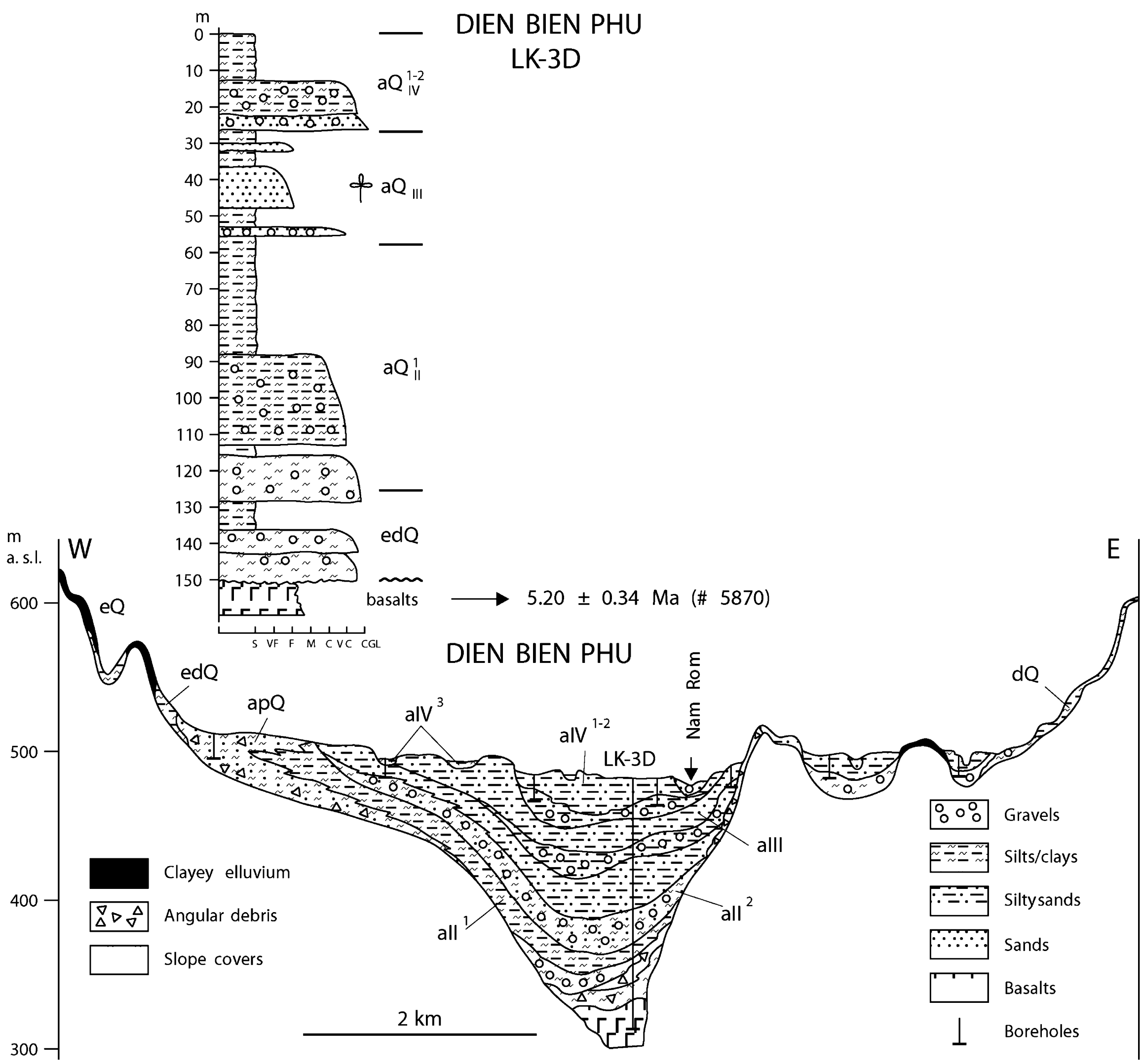


Fig. 5. Log and cross-section of the LK-3D borehole in Dien Bien Phu city (based on N.D. Dy, personal communication, 2002; see also Zuchiewicz et al., 2004), showing position of the K–Ar-dated basalt samples; cross on the lithostratigraphic log denotes finds of macrofloristic remains.

mass, showing corroded margins. Plagioclase phenocrysts (bytownite–labradorite $An_{76–66}$) occur as well-shaped forms and preserved plates (0.7–1.6 mm in size) that show repeated lamellar twinning and, rarely, oscillatory zoning. Plagioclase crystals (1 mm in diameter), that also show poorly developed oscillatory zoning, differ slightly in composition ($An_{74–64}$). A distinct increase in the albite content is restricted to the outermost zones ($An_{54}Ab_{40}Or_6$) only. Plagioclase phenocrysts are sporadically overgrown on the margins by fine rims of potassium–sodium-feldspar $Or_{71}$ (20–50 μm thick; cf. Fig. 6a). In sample LK-3D rims of K–Na-feldspar on plagioclase phenocrysts are frequent. Sieve-textured feldspar xenocrysts are very rare. They are up to 1 mm in size, and consist of plagioclase ($An_{58–40}Ab_{53–40}Or_{2–3}$) and alkali glass, showing a fine, mesh-like texture.

Phenocrysts of orthopyroxene (bronzite–hypersthene $Wo_{5–4}En_{75–53}Fs_{41–22}$) are 0.3–0.9 mm in diameter and are usually xenomorphic. Well-shaped prismatic crystals are rare. Their surfaces are clouded, due to strong alteration, and Fe–Ti oxides occur in indistinct cleavage fissures. Orthopyroxene is colourless and non-pleochroic, and often overgrown (Fig. 6b) by clinopyroxene (augite $Wo_{41–27}En_{44–32}Fs_{32–27}$; rare pigeonite $Wo_{10}En_{51}Fs_{39}$). In sample LK-3D, very fine clinopyroxene rims overgrow orthopyroxene phenocrysts. Clinopyroxene is colourless and non-pleochroic, being better preserved, although also slightly corroded. In sample VA 24, carbonate (siderite) was observed in the central parts of poorly preserved orthopyroxenes.

Olivine ($Fo_{67–55}$ in the centre of grains to $Fo_{51–46}$ on the rims) occurs as phenocrysts 1.20–0.42 mm in size. In samples VA 24 and DB 54 olivine phenocrysts are smaller, only 0.14–0.28 mm in size. They are well preserved, colourless and non-pleochroic and form xenomorphic crystals or, less commonly, automorphic plates. Alteration is indicated by iron oxides and hydrated oxides in fissures and on crystal margins. Olivine crystals are overgrown by clinopyroxene: pigeonite and augite.

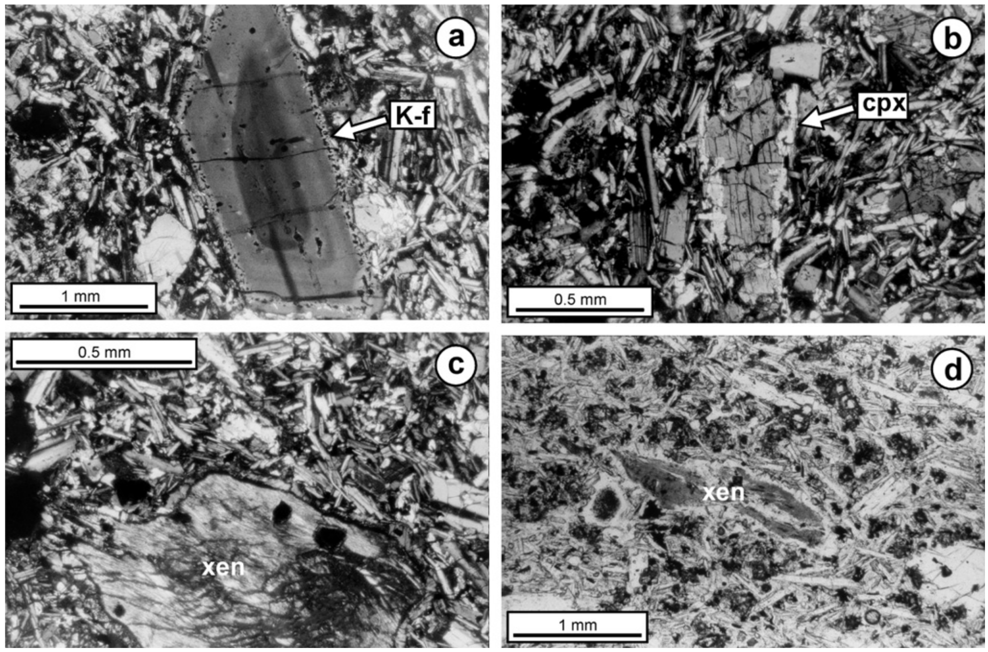


Fig. 6. Selected examples of minerals found in basalt samples DB 52, VA 24, and LK-3D: (a) subtle rims of K-feldspar around a plagioclase phenocryst (sample DB 54); crossed polars, 40×; (b) Pyroxene phenocryst: clinopyroxene overgrowing orthopyroxene (sample DB 54); crossed polars, 40×; (c) a wallrock xenolith: fibrous mat of fine-crystalline sillimanite/mullite and Mg–Fe spinel (sample DB 54); crossed polars, 90×; (d) a wallrock xenolith consisting of sillimanite/mullite and Mg–Fe spinel (sample VA 24); plane-polarized light, 90×.

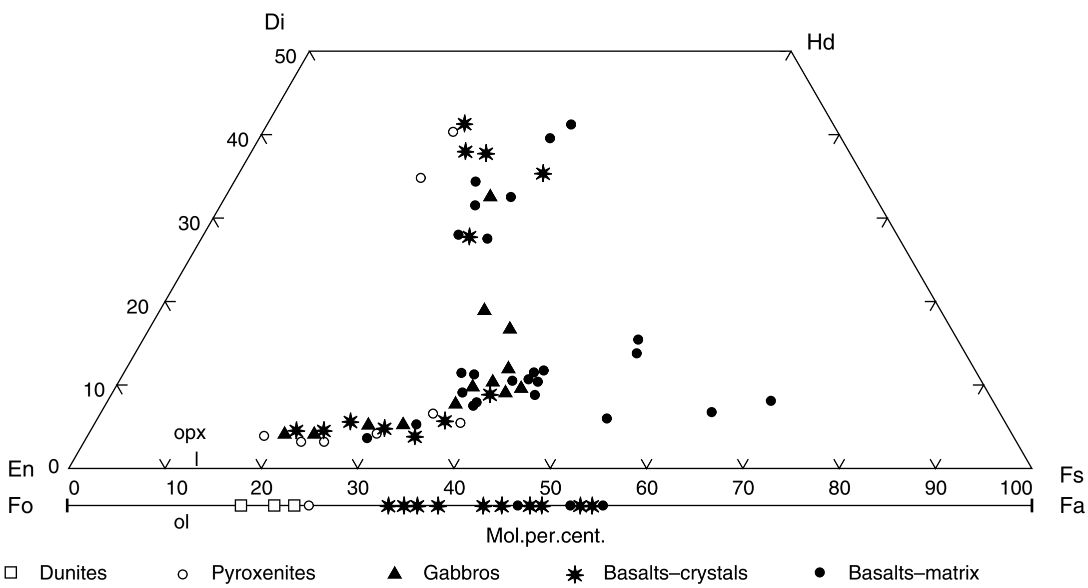


Fig. 7. Position of pyroxenes from the Dien Bien Phu basalts (samples: DB 54, VA 24, LK-3D) on the pyroxene classification diagram.

Bowlingite (a mixture of saponite, chlorite and antigorite) was not seen among the alteration products of olivine and orthopyroxene.

Alkali feldspar ($Or_{57}Ab_{27}An_{16}$) occurs rarely in these rocks in the groundmass as xenomorphic crystals within the interstices of plagioclase, pyroxene and olivine crystals.

Xenoliths (2.6–0.8 mm in size; cf. Fig. 6c and d) containing sillimanite or mullite (as suggested by EDS data) and spinel ($Mg_{58–32}$), indicate contamination by clay material and metamorphism at high temperatures as a result of contact metamorphism (sanidinite facies). Single crystals of violet spinel also occur in the groundmass (more frequently in sample DB 54).

Grains and granular aggregates of opaque minerals (Fe–Ti oxides and Fe, Ni sulphides) occur in cracks and cleavage planes, as well as on the margins of altered olivine and orthopyroxene crystals. They are also randomly dispersed in the groundmass. Vacuoles, probably left after vesicules, are filled with spherulitic siderite. These spherulites are 2.2–6.5 mm in diameter and are commonly observed in the studied rocks (e.g. samples VA 24 and DB 54).

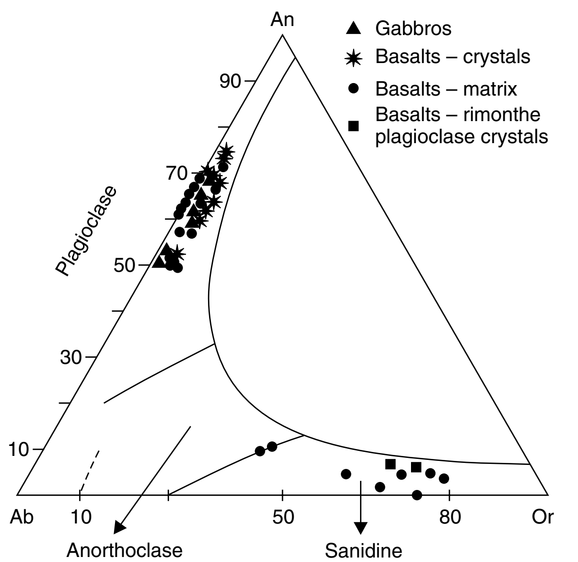


Fig. 8. Position of feldspars from the Dien Bien Phu basalts (samples: DB 54, VA 24, LK-3D) on the Ab–An–Or diagram. Symbols denote feldspar sources.

The chemical composition of pyroxenes and feldspars derived from ultramafic and mafic enclaves (pyroxenites, gabbros) and their host basalts (phenocrysts, matrix) are presented on Figs. 7 and 8. The modal composition of representative samples of the Dien Bien Phu basalts are given in Table 1. Crystallization temperatures of Mg–pigeonite (occurring as rim on olivine and orthopyroxene phenocrysts and microcrystals in DBP basalt matrix) were calculated using the method of Ishii (1975), and vary from 1089 to 1076 °C. This method is based on the chemical composition of Mg–pigeonites. This geothermometer is approximated by a line $T = 1270–480X_{Fe}$ ($T$ is temperature in degree celsius and $X_{Fe}$ is atomic ratio Fe/(Mg + Fe).

Table 1
Major and trace element compositions of the Dien Bien Phu basalts

| Major elements | VA 24 | DB 54 | LK-3 | DBP-1 Hoang et al., (1996a,b) |
|---|---|---|---|---|
| *wt%* | | | | |
| $SiO_2$ | 54.34 | 52.86 | 55.05 | 54.69 |
| $TiO_2$ | 2.08 | 1.93 | 2.17 | 2.02 |
| $Al_2O_3$ | 15.37 | 15.12 | 16.20 | 15.84 |
| $FeO_{tot.}$ | 9.27 | 10.03 | 8.30 | 9.56 |
| MnO | 0.17 | 0.19 | 0.14 | 0.16 |
| MgO | 5.06 | 4.84 | 5.14 | 5.30 |
| CaO | 6.50 | 6.14 | 6.21 | 6.09 |
| $Na_2O$ | 3.29 | 3.12 | 3.05 | 2.97 |
| $K_2O$ | 2.01 | 1.93 | 2.30 | 2.02 |
| $P_2O_5$ | 0.34 | 0.32 | 0.40 | 0.32 |
| LOI | 0.78 | 1.29 | 0.14 | 1.93 |
| Total | 99.21 | 97.77 | 99.10 | 100.90 |
| *ppm* | | | | |
| Cr | 141 | 135 | 140 | 119 |
| Ni | 105 | 95 | 87 | 110 |
| Cu | 35 | 36 | 38 | 31 |
| Zn | 134 | 117 | 130 | 113 |
| Rb | 66 | 73 | 73 | 65 |
| Sr | 319 | 300 | 347 | 287 |
| Y | 30 | 30 | 26 | 31 |
| Zr | 172 | 170 | 177 | 182 |
| Nb | 31 | 30 | 33 | 30 |
| Ba | 330 | 317 | 371 | 318 |
| Ce | 42 | 41 | 40 | 43.3 |
| La | 20.9 | 21.9 | 21 | 22.0 |
| Nd | 17 | 24 | 19 | 22.5 |
| Sm | 5.8 | 5.7 | 5.2 | 6.0 |
| Eu | 1.7 | 1.6 | 1.8 | 1.6 |
| Tb | 0.5 | 0.9 | 0.6 | 1.1 |
| Dy | | | | 6.1 |
| Yb | 2.3 | 2.4 | 2.1 | 2.1 |
| Lu | 0.32 | 0.34 | 0.3 | 0.30 |
| Hf | 4.7 | 5.3 | 4.9 | 6.0 |
| Ta | 2 | 2 | 2 | 2.0 |
| U | 1.6 | 2 | 1.3 | 1.3 |
| Th | 5.2 | 5.9 | 4.6 | 6.7 |
| Sc | 18.0 | 17.3 | 15.2 | 15.9 |
| $K_2O/Na_2O$ | 0.61 | 0.62 | 0.75 | 0.68 |
| Zr/Y | 5.73 | 5.67 | 6.81 | 5.87 |
| La/Nb | 0.67 | 0.71 | 0.64 | 0.73 |
| Rb/Sr | 0.21 | 0.24 | 0.21 | 0.23 |
| Ba/Zr | 1.92 | 1.86 | 2.10 | 1.75 |

## 5. Analytical techniques

### *5.1. K–Ar dating*

The analytical work was carried out at the Institute of Nuclear Research of the Hungarian Academy of Sciences (ATOMKI) in Debrecen, Hungary. The age of sample LK-3D was determined on magnetic mineral separates, whereas the age of sample VA-24 was measured on a whole rock sample, due to its mineralogical composition. About 1 kg of unweathered sample, free of xenoliths and joints, was crushed and sieved, grain fractions of 500–300, and 200–100 μm being used for further treatment. A whole rock split of about 30–40 g was prepared for mineral fraction separation.

Approximately 0.1 g of finely ground sample was digested in HF, then dissolved in 0.2 M HCl. Potassium was determined by flame photometry with a Na buffer, and Li international standard, as well as inter-laboratory standards Asia 1/65, LP-6, HD-B1, and GL-O. Argon was extracted from the samples by RF fusion in Mo crucibles, in a previously backed stainless steel vacuum system. The $^{38}$Ar spike was added from gas pipette system and the evolved gases were cleaned using Ti and SAES getters and liquid nitrogen traps, respectively. The purified Ar was then transported directly into the mass spectrometer, and the Ar isotope ratio was measured in the static mode, using a 15 cm radius magnetic sector-type mass spectrometer, built in Debrecen. Details regarding the instruments, the methods applied, and the results of calibration have been described by Odin (1982) and Balogh (1985).

Atomic constants suggested by Steiger and Jäger (1977) were used for calculating the ages. All analytical errors represent one standard deviation, i.e. analytical confidence level of 68%. Since we base our analytical errors on the long-time stability of the instruments, and on the deviation of our results obtained on standard samples from the interlaboratory mean, the analytical errors are likely to be overestimated.

### 5.2. Whole-rock geochemistry

Mineral shapes and compositions were examined using a scanning electron microscope (JEOL 5410), equipped with an energy dispersive spectrometer Voyager 3100 (NORAN). According to the 'standardless' procedure of calculation (i.e. using standards from the software library supplied by the manufacturer), the data were normalised to the numbers of oxygens per formula unit.

The sampled basalts (DB 54, VA 24, LK-3D) were also analysed for major and trace elements at the Activation Laboratories Ltd in Canada, by means of the following methods: ICP MS (major elements), INAA (trace elements including RE), and XRF (Nb).

#### 5.2.1. XRF pressed pellet

Trace element analyses were done on pressed powder pellets made of 6 g of a sample. Spectral interferences were corrected from pre-calculated interfering factors. Because of the trace level (<1000 ppm) of the analytes, only the mass absorptions were corrected for matrix effects. The background and mass absorption corrected intensities were then calculated against the calibrations constructed from 24 international geological reference materials. In general, the limits of detection are between 1 and 5 ppm. Samples were analysed on a Philips PW-2400 sequential XRF analyzer with Philips Super Q software.

#### 5.2.2. Trace elements by INAA

The samples were weighed into small polyethylene vials especially fabricated for ACTLABS for low background, and then irradiated with control international reference material Canmet MRG-1 and NiCr flux wires at a thermal neutron flux of $7\times10^{-12}$ n.cm$^{-2}$ s$^{-1}$ in the McMaster Nuclear Reactor. Following a 7 day decay, the samples were measured on an Ortec high purity Ge detector with a resolution of 1.67 KeV for the 1332 Co-60 photopeak. The detector is linked to Canberra Series 95 multichannel analyzer under computer control.

#### 5.2.3. Major elements by fusion ICP-OES

The samples were prepared and analysed in batches; each batch containing a method reagent blank, certified reference material and 17% replicates. Samples were mixed with a flux of lithium metaborate and lithium tetraborate and fused in an induction furnace. The molten melt was immediately poured into a solution of 5% nitric acid containing an internal standard, and mixed continuously until completely dissolved (~30 min). The samples were then run for major oxides and selected trace elements on a combination simultaneous/sequential Thermo Jarrell-Ash ENVIRO II ICP. For the ICP analysis, reagent blanks with and without the lithium borate flux were analysed, as well as the method reagent blank. Interference correction verification standards were analysed. Calibration was performed using multiple USGS and Canmet certified reference materials.

## 6. Geochronological constraints

The drilled basalts sampled at Dien Bien (LK-3D borehole; Figs. 4 and 5) underlie a nearly 130 m-thick sequence of fluvio-lacustrine-paludal sediments. These were dated using the $^{40}Ar/^{39}Ar$ method (sample DBP-1) as 5.4±0.1 Ma by Lee et al. (1998), as compared to a $^{40}K/^{40}Ar$ age of 5.20±0.34 Ma (sample LK-3D, lab. no. 5870; 1.39% K, 22.8% rad. $^{40}Ar$, $2.821\times10^{-7}$ ccSTP/g rad. $^{40}Ar$; cf. Pécskay et al., 2002; Zuchiewicz et al., 2004). A surface outcrop sample (VA-24, lab. no. 6096; 1.62% K, 24.9% rad. $^{40}Ar$), dated by one of us (Pécskay et al., 2002), yielded ages of 4.38±0.27 and 4.93±0.30 Ma, depending on the calculated amount of $^{40}Ar$ ($2.762\times10^{-7}$ ccSTP/g rad. $^{40}Ar$ and $3.109\times10^{-7}$ ccSTP/g rad. $^{40}Ar$, respectively).

Our K–Ar age determinations point to an Early Pliocene (Zanclean) age (Harland et al., 1989; Palmer and Geissman, 1999) for the basaltic magmatism in the DBPFZ, falling between 4.4 and 5.2 Ma. Since, the misinterpretation of the measurements due to 'excess argon' or diffusion deficiency cannot be excluded, particularly in some of the subvolcanic rocks, more detailed analytical work will be required.

## 7. Geochemistry

Basalts from the Dien Bien Phu area differ from other Vietnamese basalts in several respects. The $SiO_2$ contents in the DBP basalts are relatively high, ranging from 52–55 wt%, with low MgO (5.0 wt%) and $FeO_{total}$ up to 9 wt%, and $TiO_2$ contents of ca. 2 wt%, characterising them as high-titanium basalts. Aside from $FeO_{total}$ which varies from 8.3 (LK-3D) to 10.0 wt% (DB-54) (Table 1), the major element contents are similar in all the samples collected. With regard to trace elements, the LK-3D sample is enriched in Sr (347 ppm) and Ba (371 ppm), and also shows the highest $K_2O/Na_2O$ ratio (0.75), as compared to the other DBP basalt samples (0.61–0.62). Other trace elements, including REE, show little or no significant variation (Tables 1 and 2).

On the TAS diagram (Le Maitre et al., 1989), the Dien Bien Phu data plot in the field of basaltic andesite, close to the boundary with that of basaltic trachyandesite. This is in contrast to other Vietnamese quartz tholeiites (Hoang et al., 1996a,b; Hoang and Flower, 1998), which conform to the basaltic andesite and basalt fields (Fig. 9). In the $K_2O/SiO_2$ diagram, the Dien Bien Phu basalts conform to high-K calc-alkaline composition, the contents of $FeO_{total}$, $Na_2O + K_2O$ and MgO (AFM diagram; cf. Irvine and Baragar, 1971) also corresponding to the calc-alkaline series. In the Nb/Y–Zr/$TiO_2$ diagram of Winchester and Floyd (1977), however, Vietnamese basalt data plot invari-

Table 2
Incompatible trace element ratios in the crustal and mantle reservoirs, according to data cited by Rollinson (1993) cf. also Saunders et al. (1988) and Weaver (1991). DBP-1 after Hoang et al. (1996a); VA 24, DB 54, LK-3D-this paper

| | Zr/Nb | La/Nb | Ba/Nb | Ba/Th | Rb/Nb | K/Nb | Th/Nb | Th/La | Ba/La |
|---|---|---|---|---|---|---|---|---|---|
| Primitive mantle | 14.8 | 0.94 | 9.0 | 77 | 0.91 | 323 | 0.117 | 0.125 | 9.6 |
| N-MORB | 30 | 1.07 | 1.7–8.0 | 60 | 0.36 | 210–350 | 0.025–0.071 | 0.067 | 4.0 |
| Continental crust | 16.2 | 2.2 | 54 | 124 | 4.7 | 1341 | 0.44 | 0.204 | 25 |
| HIMU OIB | 3.2–5.0 | 0.66–0.77 | 4.9–6.9 | 49–77 | 0.35–0.38 | 77–179 | 0.078–0.101 | 0.107–0.133 | 6.8–8.7 |
| EMI OIB | 4.2–11.5 | 0.86–1.19 | 11.4–17.8 | 103–154 | 0.88–1.17 | 213–432 | 0.105–0.122 | 0.107–0.128 | 13.2–16.9 |
| EMII OIB | 4.5–7.3 | 0.89–1.09 | 7.3–13.3 | 67–84 | 0.59–0.85 | 248–378 | 0.111–0.157 | 0.122–0.163 | 8.3–11.3 |
| VA 24 | 5.55 | 0.67 | 10.65 | 63.5 | 2.13 | 539 | 0.17 | 0.25 | 15.8 |
| DB 54 | 5.67 | 0.73 | 10.57 | 53.7 | 2.42 | 533 | 0.20 | 0.27 | 14.5 |
| LK-3D | 5.36 | 0.64 | 11.24 | 80.7 | 2.21 | 578 | 0.14 | 0.22 | 17.7 |
| DBP-1 | 6.07 | 0.73 | 10.60 | 47.5 | 2.17 | 560 | 0.22 | 0.30 | 14.5 |

According to the data cited by Rollinson (1993); cf. also: Saunders et al. (1988) and Weaver (1991); DBP-1 after Hoang et al. (1996a); VA 24, DB 54, LK-3D-in this paper

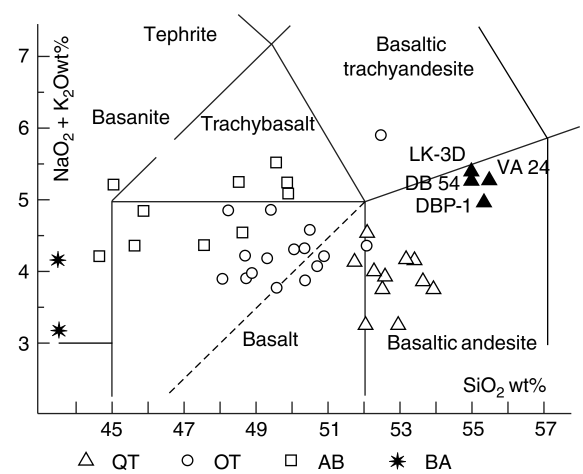


Fig. 9. Plots of the Dien Bien Phu basalts on the TAS diagram. Dien Bien Phu basalts shown by triangles; the other data taken from Hoang et al. (1996a) and Hoang and Flower (1998).

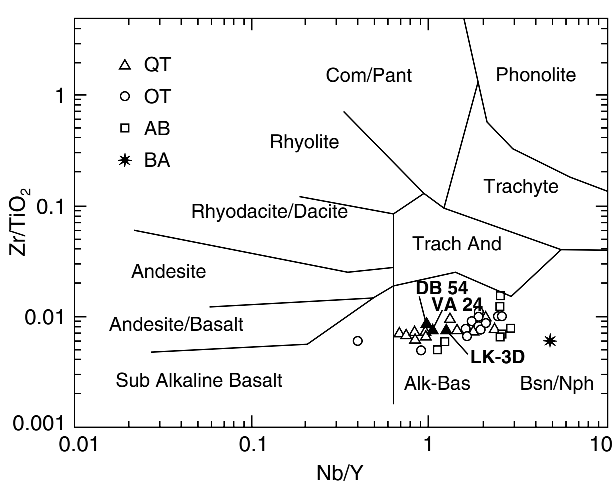


Fig. 10. Plots of the Dien Bien Phu basalts compared with other Vietnamese Cenozoic basalts quoted by Hoang et al. (1996a) on the Zr/$TiO_2$ vs. Nb/Y diagram (Winchester and Floyd, 1977); *-sample DBP-1.

ably within the alkali basalt field (Fig. 10), whereas in the CIPW normative projection (nepheline–olivine–diopside–hypersthene–quartz diagram; after Thompson, 1984), the data for DBP plot in the field of quartz tholeiite. In the Meschede (1986) diagram, moreover, the data conform to within-plate alkali basalts and tholeiites (Fig. 11).

## 8. Discussion

### *8.1. Position of the Dien Bien Phu basalts in the light of tectonic constraints on the Late Neogene volcanism in Vietnam*

Hoang and Flower (1998) propose a 'diffuse volcanic province' which has resulted from the combined effect of lithosphere transtension and asthenosphere decompression, coeval with collision-induced extrusion of thermally anomalous mantle. Several authors consider that the compositions of late Cenozoic basalts in Vietnam are indicative of upwelling asthenosphere in a tensional stress regime (Hoang et al., 1996a,b; Hoang and Flower, 1998; Cung et al., 1998). Rangin et al. (1995) propose that Late Neogene volcanism in Indochina reflects synchronous E–W extension across the region, while Lee et al. (1998) conclude that Middle Miocene eruptive centres in South Vietnam migrated northwards in the Late Miocene, turning to the south in Late Pliocene time, accompanied by scattered eruptions in the north. This pattern of migration is considered by Lee et al. (1998) to record the clockwise rotation of transtensional features (Lee et al., 1998), associated with the change from left- to right-lateral motion along the Red River Fault Zone (Leloup et al., 1995). In sum, extensional axes progressed from NE–SW, following spreading in the South China Sea south-western subbasin, through NW–SE, to N–S at present (Hoang and Flower, 1998; Lee et al., 1998). An extensional tectonic regime continues to the present day (cf. Ile des Cendres).

Age equivalents of the Dien Bien Phu quartz tholeiites (4.4–5.4 Ma), among the basalts in the region, include alkali basalts at Pleiku (4.8 Ma) and Buon Ma Thuot (4.5–4.6 Ma). On the other hand, quartz tholeiites appear to be confined to age interval of 15 Ma (Phuoc Long) to 0.35 Ma (Con Co; cf. Hoang and Flower, 1998). Early

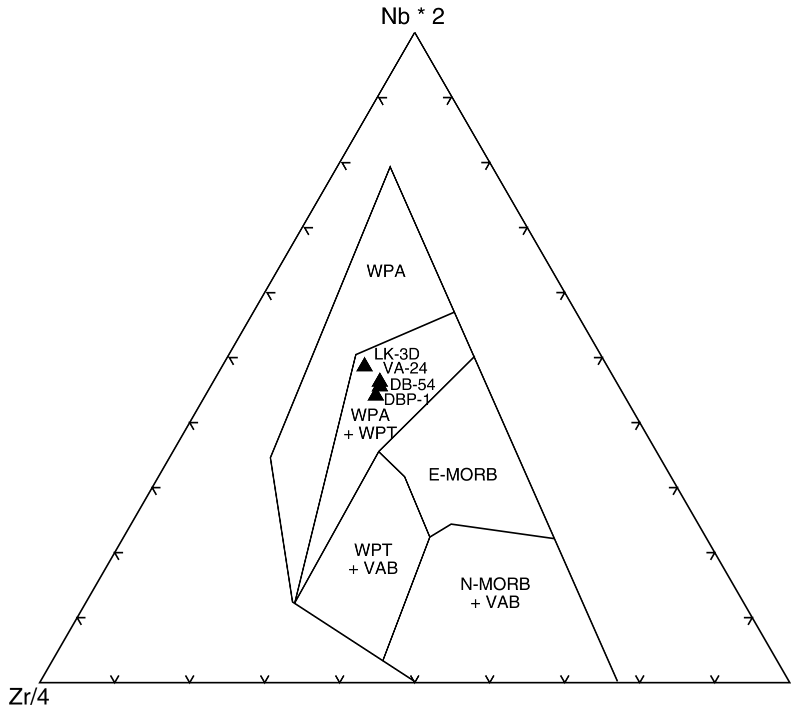


Fig. 11. Plots of Dien Bien Phu basalts on the Zr/4–2Nb–Y diagram (Meschede, 1986). The fields are defined as follows: WPA-intraplate alkali basalts, WPT-intraplate tholeiites, VAB-volcanic-arc basalts, E-MORB-E-type MORB, N-MORB-N-type MORB.

series eruptives include quartz tholeiites from Dalat, dated to 10.5–14.0 Ma (Hoang and Flower, 1998).

In common with Dien Bien Phu basalts, quartz tholeiites are dominant in the earlier Phuoc Long and Dalat series in South Vietnam, and are also present in Pleiku, Buon Ma Thuot, and Dien Bien Phu eruptive centres (Hoang and Flower, 1998), showing similarly high-$SiO_2$ and low FeO* contents (Hoang et al., 1996a,b; Hoang and Flower, 1998), tapping a relatively refractory lithosphere-like source. This may indicate that, despite their young age, the basalts probably reflect a thinned crust underlain by a hot asthenospheric plume in NW Vietnam (Hoang et al., 1996a,b; Hoang and Flower, 1998).

Regarding the intra-plate origin of Neogene basaltic magmatism in this area, we are inclined to accept Flower et al.'s (1998) model of the India/Asia collision-induced extrusion of the asthenospheric mantle, which led to lithosphere escape and the opening of the South China Sea marginal basin, providing thereby the thermal energy necessary for extension-related basaltic magmatism. Lithospheric extension alone is not the only cause of mantle melting (Flower et al., 2004). It has recently been accepted that lateral displacement of asthenospheric mantle during and after continental plate collisions in the Tethyan realm are responsible for widespread, nonplume intracontinental magmatism in southeastern Asia (cf. Flower and Coban, 2002; Flower et al., 2004).

### *8.2. T-P conditions of the DBP basalt melt crystallization*

The Dien Bien Phu quartz tholeiites are moderately phyric ( < 10%) and, apart from phenocrysts of olivine ($Fo_{67–47}$) and plagioclase ($An_{70–66}$), contain phenocrysts of orthopyroxene $En_{75–63}Fs_{22–32}Wo_{4–5}$, in contrast to the quartz tholeiites from Dalat and Phuoc Long, which are generally aphyric to moderately phyric, bearing olivine ($Fo_{78–74}$), augite ($Wo_{47–49}En_{40–36}Fs_{13–14}$), and plagioclase ($An_{83–72}$), and petrographically resemble mid-ocean ridge basalts (MORB) (Hoang et al., 1996a,b).

The presence of moderately Fe-rich olivine ($Fo_{67–55}$), together with orthopyroxene ($Wo_4En_{75–71}Fs_{25–22}$–$Wo_{5–4}En_{65–53}Fs_{41–30}$) phenocrysts in the DBP basalts, indicates $SiO_2$-saturation or oversaturation. Experimental investigations of synthetic systems, such as $Mg_2SiO_4$–$SiO_2$ (Chen and Presnall, 1975) show that peritectic melting of mantle peridotite is favoured by low pressures ( < ca.10 Kbar) and high partial pressure of water ($P_{H_2O}$), while eutectic melting occurs at higher pressures and in anhydrous conditions. Studies of the system MgO–$SiO_2$–$H_2O$ (Kitahara et al., 1966) have shown that enstatite crystallizes at temperatures above 700 °C and water vapour pressures around 345 bar, and may be stable in the presence of water to approximately 900 °C. On the other hand, Carlson's (1988) investigations under atmospheric pressure conditions suggest that enstatite is stable below ~1000 °C in the presence of water.

Kushiro (1990) showed that the presence of orthopyroxene phenocrysts is characteristic of calc-alkaline rather than MORB tholeiite, as observed in basalts associated with island arcs, active continental margins and back-arc basins (Wilson, 1993). Hoang and Flower (1998) note that orthopyroxene–phyric tholeiites are highly unusual in intraplate tectonic settings and that their presence may reflect relatively high ($P_{H_2O}$) in their mantle source. An alternative explanation is that orthopyroxene crystallized from magmas that have assimilated crustal sedimentary rocks.

As already noted, microcrystals of Fe-rich pigeonite ($Wo_{16–6}En_{55–42}Fs_{53–35}$) together with augite are recorded in the matrix of the DBP basalts. The presence of pigeonite in continental basalts may indicate that the magma has been variably contaminated by continental crust on its route to the surface (Campbell, 1985; Deer et al., 1992).

Crystallization temperatures of Mg-pigeonites (1080±10 °C at 1 atm pressure) in the DBP basalts were calculated using the Mg–pigeonite geothermometer (Ishii, 1975). These temperatures correspond to late crystallization stages represented by microcrysts of pigeonite formed as overgrowths on olivine and orthopyroxene phenocrysts. Melt segregation pressures and temperatures inferred for Vietnamese quartz tholeiites under hydrous conditions have been estimated at 1128±14l °C at 5 kbar (Hoang et al., 1996b), or 1350–1400 °C at 1.5 GPa (Hoang and Flower, 1998).

### 8.3. Geochemical aspects of crustal contamination

From their incompatible element ratios, Hoang and Flower (1998) concluded that some Vietnamese basalt had undergone contamination by crustal material. Crustal contamination can affect mantle-derived melts after they have left their source region (Hawkesworth and van Calsteren, 1983) or in the mantle source region itself, the latter as a result of subducted sediment (Rollinson, 1993).

The extent of either type of contamination in continental basalts is controversial (e.g. Carlson, 1991; Hergt et al., 1991; Arndt et al., 1993), and is difficult to identify on the basis of rock geochemistry alone, even if the chemical compositions of both contaminant and magmatic sources are known independently (e.g. Carlson and Hart, 1988; Barling et al., 1994).

Huppert and Sparks (1985) indicate the following mechanisms for the interaction of mantle-derived magmas with crustal rocks:

1. Mixing of crustal and mantle partial melts in magma chambers or conduits.
2. Contamination by small-fraction melts from walls, roof or floor of the magma chamber or conduits.
3. Assimilation by the stoping of crustal blocks (bulk assimilation).

In general, the mixing of crustal components and basalt magmas (or their source regions) modifies the geochemistry of their incompatible elements, as reflected, for example, by positive covariance of $^{87}Sr/^{86}Sr$ with such parameters, as: $SiO_2$, Rb/Sr, $K_2O/P_2O_5$, Ba/Nb, and La/Nb (Thompson, 1984; Carlson and Hart, 1988; Fitton et al., 1988), as well as La/Ta and Th/Ta (Loubet et al., 1988). De Paolo (1981) has shown that assimilation in magma chambers is commonly associated with concurrent fractional crystallization (AFC processes). Consequently, the above-mentioned relationships can be complicated by these AFC processes, as well by the effects of partial melting.

The incompatible element compositions of the DBP basalts are distinct in certain respects (e.g. Rb/Nb, K/Nb, Th/Nb, and Th/La) from the other Vietnamese basalts, although other element ratios (as Zr/Nb, La/Nb, Ba/Nb, Ba/Th and Ba/La) are comparable. The values of Rb/Nb, K/Nb, Th/Nb, and Th/La are higher than those of EM2-rich OIB, and are intermediate between the latter and those of the continental crust (Table 2).

In general, Vietnamese basalts show Rb/Sr ratios ranging from 0.02–0.11, with the exception of those from the southwestern unit, which have Rb/Sr ratios up to 0.18. In the Dien Bien Phu basalts, whole Rb/Sr ratios exceed 0.2 (0.21–0.24; cf. Fig. 12). In contrast, the Zr/Ba ratio (0.48–0.57) is lower than 0.8; a feature characteristic of the other basalts. Similarly, it is clear from the Ta/La vs. Th/La diagram (Fig. 13) that the DBP basalts have a significantly higher Th/La ratios ( > 0.22) than those of other Vietnamese basalts, which do not exceed 0.2.

According to Hoang and Flower (1998), increased ratios, such as: Rb/Zr, and Ba/Zr vs. Ti/Zr reflect the addition of crustal components. In the Dien Bien Phu basalts only Rb/Zr and Ti/Zr increase significantly, while Ba/Zr and Ti/Zr are close to the average for the other basalts. Otherwise large ion, lithophile element contents (LILE) such as Rb, K and Th, are relatively enriched but depleted in Ba. It is clear from the DBP compositions (Fig. 14) that incompatible element distributions (normalized to average primitive mantle; McDonough et al., 1992) resemble oceanic island basalts (OIB) rather than MORB, and show positive K and Th anomalies, and negative anomalies of Ba and Nb. Similarly, there are significant differences from

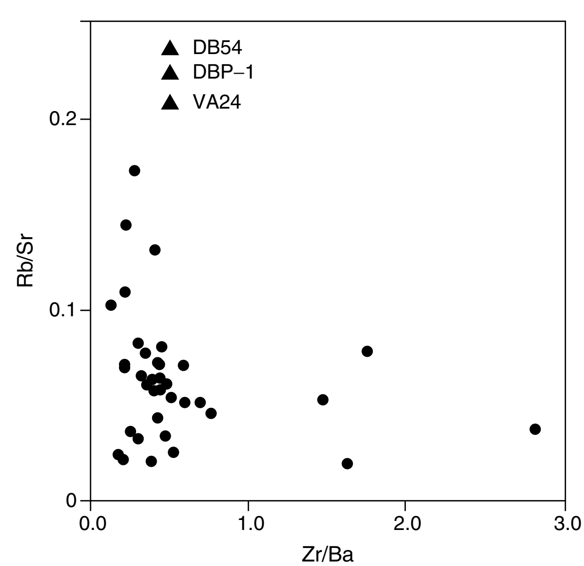


Fig. 12. Rb/Sr vs. Zr/Ba diagram for the Dien Bien Phu basalts, compared with other Vietnamese Cenozoic basalt data of Hoang et al. (1996a,b).

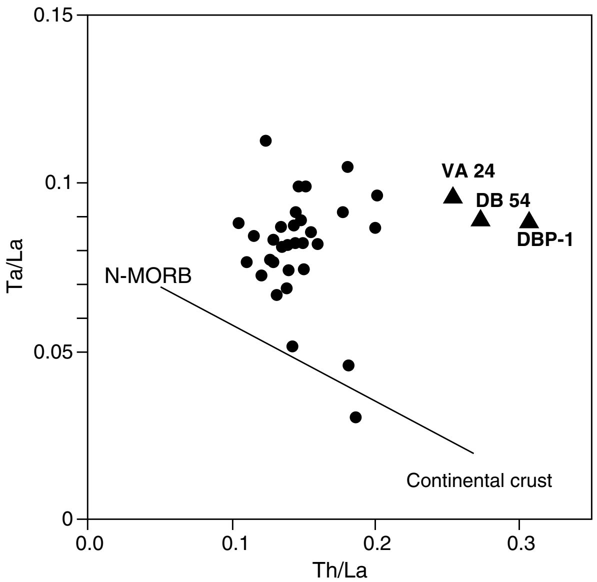


Fig. 13. Ta/La vs. Th/La diagram for the Dien Bien Phu basalts, compared with other Vietnamese Cenozoic basalt data of Hoang et al. (1996a,b).

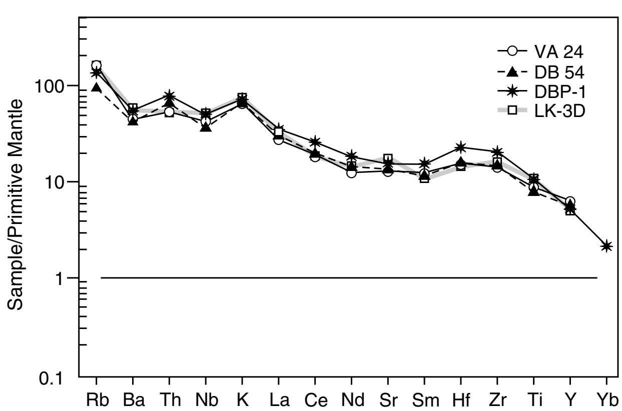


Fig. 14. Spider diagram showing primitive mantle-normalized incompatible element distributions for the Dien Bien Phu basalts.

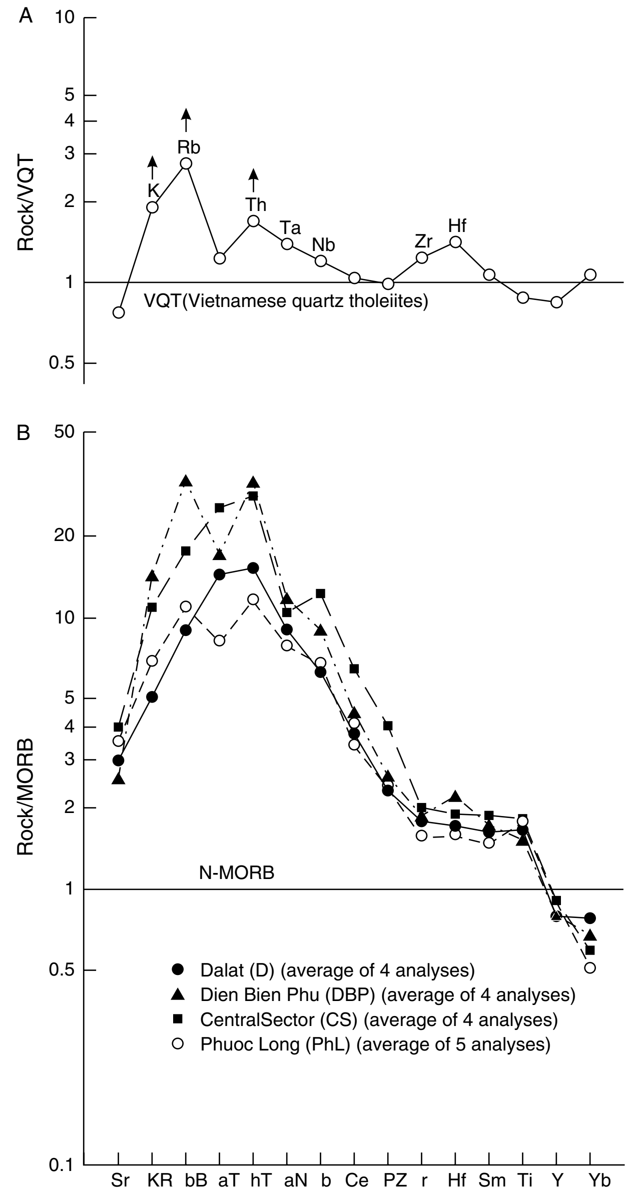


Fig. 15. Some geochemical characteristics of Cenozoic basalts in Vietnam: (a) Vietnamese quartz tholeiites (VQT)-normalized trace element variation diagram for quartz tholeiites from Dien Bien Phu. Data of VQT chemical analyses have been taken from Hoang and Flower (1998); (b) MORB-normalized trace element variation diagram (Pearce and Cann, 1973) for quartz tholeiites from various regions of Vietnam. Data of Dalat, Phuoc Long, and the central sector have been taken from Hoang and Flower (1998).

other Vietnamese quartz tholeiites (Fig. 15). Among the most mobile elements: K, Rb, Sr and Ba, two-K and Rb-are significantly enriched in the DBP basalts, while of the immobile elements Th–Yb are the most enriched. Th. Ta, Nb, Zr and Hf are enriched to a lesser degree, whereas Ti and Y show slight depletion, in these respects resembling other Vietnamese quartz tholeiites (Fig. 15).

If continental and oceanic tholeiites are generated by similar degrees of partial melting, the Vietnamese quartz tholeiites clearly do not reflect a normal MORB mantle source. Instead, their normalised distribution patterns are typical of OIB-like continental basalts. In light of this similarity, Thompson (1984) suggested that CFB tholeiites originated from magmas geochemically similar to OIB, variably contaminated by continental crust (Tables 3 and 4).

The $^{87}Sr/^{86}Sr$ ratios of 0.7065 in the Dien Bien Phu basalts are the highest recorded in Vietnamese basalts (Hoang et al., 1996a), although relatively high values also characterise basalts from Pleiku, Song Cau and Xuan Loc. Hoang et al. (1996a) suggested that this feature could reflect crustal contamination, although they were not able to distinguish whether the high $^{87}Sr/^{86}Sr$ ratios in DBP basalts represented partial melts of contaminated lithospheric mantle, or products of crustal wallrock reaction. In either case, the depletion/enrichment history of the lithospheric mantle appears to be different from that of the asthenospheric source. While the presence of EM2 can be explained fairly simply in terms of sediment subduction during previous evolution of the Eurasian-Pacific margin,

Table 3
Modal composition of the Dien Bien Phu basalts (in vol%)

| | DB 54 lava flow | VA 24 lava flow | LK-3D borehole |
|---|---|---|---|
| *Phenocrysts* | | | |
| Olivine | 1.5 | 1.5 | 2.0 |
| Orthopyroxene | 2.2 | 2.2 | 2.3 |
| Plagioclase | 9.4 | 7.7 | 3.6 |
| Matrix | 83.4 | 85.5 | 88.4 |
| *Rock fragments* | | | |
| Dunites | – | – | 0.4 |
| Pyroxenites | 0.3 | 0.7 | 0.3 |
| Gabbros | 2.9 | 2.1 | 1.2 |
| Xenoliths of sedimentary rocks | 0.3 | 0.3 | 1.8 |
| Total | 100.0 | 100.0 | 100.0 |

the provenance of asthenospheric EM1 and its apparent absence from the lithospheric mantle remain problematic (Hoang et al., 1996a,b).

### *8.4. Contamination processes in the DBP basalts*

Crustal contamination is thus clearly indicated by the increased ratios of some incompatible elements in the basalts, whether in mantle source material or as an effect of magma reaction with wallrock.

In the case of the Dien Bien Phu basalts, the presence of very small xenoliths of country rock (siltstone and claystone) is a critical clue that at least some contamination, occurred during magma ascent. Accordingly, the eruption of basalts through sedimentary rocks suggests trapping and assimilation of small fragments, several millimetres in size. High magmatic temperatures were responsible for the structural transformation of xenolith mineral phases; clay minerals being altered to sillimanite/mullite and spinel at temperatures exceeding 900 °C and low pressure (sanidinite facies). Mobile elements, such as potassium, appear to have migrated, forming K-feldspar in the volcanic groundmass.

It can be assumed that the melt was similarly enriched in other elements contained in the xenoliths. The presence of xenoliths of country rocks in the basalts could, to some degree, influence their chemical composition, but would be expected to result in selective changes of their incompatible element parameters. It may be assumed that an additional, or possibly equally important, factor was the contamination of magma by mobile elements originating from the wallrocks. Patchett (1980) observed that magmas can be selectively contaminated by elements derived from hydrous fluids, released by the dehydration of heated wall rocks. According to Watson (1982), the transfer of alkali elements, such as potassium, reflects their much greater chemical diffusivity.

In the DBP region, the sedimentary rocks surrounding the basalts contain both water and alkali elements. During magma migration, selective mobilization of potassium and rubidium, two of the most mobile elements, could have taken place, enriching the residual basaltic melt (Saunders et al., 1988; Rollinson, 1993). Consequently, their enrichment of DBP basalts and abnormally high K/Rb ratios can be explained by this process, in addition to the observed presence of K-feldspar rims on plagioclase phenocrysts and enhanced $^{87}Sr/^{86}Sr$ isotopic ratios.

Table 4
Petrographic and mineralogical characteristics of studied Dien Bien Phu basalts

| | DB54 lava flow | VA 24 lava flow | LK–3D borehole |
|---|---|---|---|
| *Phenocrysts* | | | |
| Olivine | Hyalosiderite (core) $Fo_{67–62}$ hortonolite (rim) $Fo_{51–47}$ 0.21–0.28 mm in size overgrown by: pigeonite $Wo_9En_{55}Fs_{36}$ augite $Wo_{38}En_{38}Fs_{24}$ | Hyalosiderite (core) $Fo_{55}$ 0.14–0.15 mm in size overgrown by augite $Wo_{38}En_{40}Fs_{21}$ | Hyalosiderite (core) $Fo_{65–57}$ hortonolite (rim) $Fo_{46}$ 0.42–1.20 mm in size |
| Orthopyroxene | Bronzite $Wo_4En_{73–72}Fs_{24–23}$ 0.21–0.96 mm in size overgrown by: pigeonite $Wo_{10}En_{51}Fs_{39}$ augite $Wo_{34–27}En_{44–39}Fs_{29–26}$ | Bronzite $Wo_4En_{75–71}Fs_{34–22}$ hypersthene $Wo_5En_{63–53}Fs_{36–32}$ 0.28–0.35 mm in size overgrown by augite $Wo_{37}En_{40}Fs_{23}$ | Bronzite $Wo_4En_{71}Fs_{25}$ hypersthene $Wo_4En_{65–55}Fs_{41–30}$ 0.56–0.70 mm in size overgrown by: pigeonite $Wo_5En_{68}Fs_{27}$ augite $Wo_{41–37}En_{38–32}Fs_{32–21}$ |
| Plagioclase | Labradorite $An_{67–66}Ab_{39–30}Or_4$ 0.32–1.06 mm in size overgrown by alkali feldspar $Ab_{39}Or_{55}An_6$ | Labradorite $An_{66–64}Ab_{32–31}Or_{4–3}$ 0.28– 0.92 mm in size overgrown by alkali feldspar $Ab_{29}Or_{66}An_5$ | Bytownite (core) $An_{74}Ab_{24}Or_2$ labradorite (rim) $An_{69–52}Ab_{43–28}Or_{6–3}$ 0.70–1.55 mm in size overgrown by alkali feldspar $Ab_{22}Or_{73}An_5$ |
| *Matrix* | | | |
| Olivine | Hortonolite $Fo_{37}$ 0.03 mm in size | Hortonolite $Fo_{48–45}$ 0.03 mm in size | Hortonolite $Fo_{47}$ 0.07 mm in size |
| Clinopyroxene | Pigeonite $Wo_{10–9}En_{55–44}Fs_{47–35}$ augite $Wo_{33–32}En_{42–39}Fs_{27–25}$ 0.06 mm in size | Pigeonite $Wo_{16–6}En_{55–42}Fs_{53–36}$ augite $Wo_{42–30}En_{42–30}Fs_{32–28}$ 0.04 mm in size | Pigeonite $Wo_{10}En_{47}Fs_{43}$ augite $Wo_{34}En_{41}Fs_{25}$ 0.07 mm in size |
| Plagioclase | Labradorite $An_{66–57}Ab_{39–29}Or_{4–1}$ 0.02–0.13 mm in size | Labradorite $An_{63–60}Ab_{39–36}Or_1$ 0.01–0.14 mm in size | Bytownite $Ab_{27–22}An_{76–71}Or_2$ labradorite $An_{57–51}Ab_{46–39}Or_{5–3}$ 0.03–0.08 mm in size |
| K-feldspar | Sanidine $Or_{78–75}Ab_{25–18}An_5$ < 0.01 mm in size | Sanidine $Or_{75}Ab_{21}An_5$ < 0.01 mm in size | Sanidine $Or_{75–60}Ab_{36–21}An_{5–4}$ < 0.01 mm in size |
| Country rocks xenoliths | Spinel $Mg_{58}$ sillimanite/mullite 0.65 × 1.90 mm in size | Spinel $Mg_{43–41}$ sillimanite/mullite 0.21 × 0.75 mm in size | Spinel $Mg_{42}$ sillimanite/mullite 0.36 × 2.60 mm in size |

#### 8.4.1. Influence of contamination processes on chemical composition of the Dien Bien Phu basalts

As already mentioned, the Dien Bien Phu basalts probably reflect two types of contamination: by assimilation of sedimentary wallrock material, and by selective enrichment in mobile elements derived from these wallrocks and mobilized by hydrous fluids.

Given the nature of the wallrock, the chemistry of DBP basalts could have affected both the content of alkalis and also other elements, mainly silica. The amount of preserved metamorphic xenoliths is below 2 vol% was probably an indicator of their fine-grained character, given the likelihood that the primary assimilated material exceeded such values.

Despite the relatively high $SiO_2$ values (more typical of andesite), the relatively low $Zr/TiO_2$ ratios indicate that these rocks were originally basaltic which were later enriched in $SiO_2$. Even small increases in the concentrations of $SiO_2$ and $K_2O$ would affect the projected compositions of these rocks in classification diagrams based on such elements. For example, in the TAS diagram, these compositions are displaced from the basalt to the basaltic andesite field; while in that of Thompson (1984), based on normative CIPW composition, the compositions are shifted from the olivine tholeiite to the quartz tholeiite field. Taking into account the above-mentioned contamination processes, the most appropriate classification diagram is that of Winchester and Floyd (1977) based on the contents of immobile incompatible trace elements (Nb, Y, Zr, Ti).

The petrographic character of the DBP basalts (olivine, orthopyroxene and plagioclase phenocrysts, and lack of silica glass or quartz in the groundmass) also suggests that these rocks were originally olivine- rather than quartz tholeiites (Tables 3 and 4).

## 9. Conclusions

1. Rapid migration of basaltic magma to the surface in the Dien Bien Phu Fault Zone is documented by structural and textural features and probably reflects recent transtension of the crust in this region, combined with asthenospheric upwelling, possibly induced by lateral mantle displacement. Geochemical signatures indicate the rocks studied are of 'within-plate' type, whose $K^{40}/Ar^{40}$ isotopic ages correspond to the Early Pliocene (4.4–4.9 and 5.4–5.2 Ma).
2. Judging from the presence of reacted olivine crystals, and the lack of quartz in the groundmass formed under $H_2O$-undersaturated conditions, the basalts are $SiO_2$–saturated/oversaturated olivine tholeiites.
3. The presence of xenoliths containing sillimanite/mullite in the DBP basalts suggests contamination of the basaltic magma by crustal wallrock material.
4. This conclusion is reinforced by presence of K-feldspar rims on plagioclase phenocrysts and in the groundmass, selective increases in incompatible element ratios indicating melt modification by assimilation of mobile elements from country rock.
5. The Dien Bien Phu basalts, classified on the basis of normative compositions, are quartz tholeiites but could, in fact, represent primary olivine basalts, modified by contamination by crustal wallrock.

## Acknowledgements

This study was supported by the State Committee for Scientific Research of Poland (KBN) through a grant no. 6 PO4E 026 18 (to W. Zuchiewicz). We extend our thanks to Dr A. Swierczewska and Prof. A.K. Tokarski who provided us with the basalt sample VA 24, Dr N.D. Dy for his description of the Dien Bien borehole log and providing the sample LK-3D. Prof. W. Narebski is thanked for critical reading of a first draft of this paper. Thoughtful reviews by Profs. J. Winchester and M. Flower have been most helpful. Dr L. Chudzikiewicz prepared the computer-generated artwork. His help is gratefully acknowledged.

## References

Anczkiewicz, R., Viola, G., Cuong, N.Q., Chi, C.T., 2000. Structural and fission-track study of the Red River shear zone in N-Vietnam. In: Cocks, R. (Ed.), Abstracts, Geoscience 2000. University of Manchester, 17–20 April 2000. Geological Society London, Manchester, p. 123.

Arndt, N.T., Czamanske, G.K., Wooden, J.L., Fedorenko, V.A., 1993. Mantle and crustal contributions to continental flood volcanism. Tectonophysics 223, 39–52.

Balogh, K., 1985. K–Ar dating of Neogene volcanic activity in Hungary. Experimental Technique, Experiences, and Methods of Chronological Studies. ATOMKI Reports D/1, Debrecen, pp. 277–288.

Barling, J., Goldstein, S.L., Nichols, I.A., 1994. Geochemistry of Heard Island (Southern Indian Ocean): characterization of an enriched mantle component and implications for enrichment of the sub-Indian Ocean mantle. Journal of Petrology 35, 1017–1053.

Briais, A., Patriat, Ph., Tapponnier, P., 1993. Updated interpretation of magnetic anomalies and seafloor spreading stages in the south China Sea: implications for the Tertiary tectonics of southeast Asia. Journal of Geophysical Research B 4 98, 6299–6328.

Campbell, I.H., 1985. The difference between oceanic and continental tholeiites: a fluid dynamic explanation. Contributions to Mineralogy and Petrology 91, 37–43.

Carlson, W.D., 1988. Subsolidus phase equlibria on the forsterite saturated join $Mg_2Si_2O_6$–$CaMgSi_2O_6$ at atmosphere pressure. American Mineralogist 73, 232–241.

Carlson, R.W., 1991. Physical and chemical evidence on the cause and source characteristics of flood basalt volcanism. Australian Journal of Earth Sciences 38, 525–544.

Carlson, R.W., Hart, W.K., 1988. Flood basalt volcanism in the northwestern United States. In: Macdougal, J.D. (Ed.), Continental Flood Basalts. Kluwer Academic Publishers, Dordrecht (Hingham, MA), pp. 35–61.

Chen, C.H., Presnall, D.G., 1975. The system $Mg_2SiO_4$–$SiO_2$ at pressures up to 25 kilobars. American Mineralogist 60, 398–406.

Cung, T.C., Dorobek, S., Richter, C., Flower, M., Kikawa, E., Yem, N.T., McCabe, R., 1998. Paleomagnetism of late Neogene basalts in Vietnam and Thailand: implications for the post-Miocene tectonic history of Indochina. In: Flower, M. (Ed.). Mantle Dynamics and Plate Interactions in East Asia. American Geophysical Union, Geodynamics Series 27, 289–299.

Cuong, N.Q., Zuchiewicz, W., 2001. Morphotectonic properties of the Lo River fault near Tam Dao in north Vietnam. Natural Hazards and Earth System Sciences 1, 15–22.

De Paolo, D.J., 1981. Trace element and isotopic effects of combined wallrock assimilation and fractional crystallization. Earth and Planetary Sciences Letters 53, 189–202.

Deer, W.A., Howie, R.A., Zussman, J., 1992. An Introduction to the Rock-forming Minerals, second ed. Geological Society, London, 696 pp.

Dy, N.D., Tu, D.V., Thuan, D.V., Tan, M.T., 1999. Relationship between Quaternary sedimentation and landslide-mudflow formation in NW Vietnam. Journal of Geology, Series B 13/14, 256–261 (Hanoi).

Fitton, J.G., James, D., Kempton, P.D., Ormerod, D.S., Leeman, W.P., 1988. The role of lithospheric mantle in the generation of late Cenozoic basic magmas in the western United States. Journal of Petrology, 331–349 (Special Lithosphere Issue).

Flower, M.F.J., Coban, H., 2002. Clues for collision-induced mantle flow from igneous activity in Anatolia and Indochina. In: IGCP 430 second Annual Workshop 'Mantle Responses to Tethyan Closure', April 1–10, 2002, Halong Bay City, Vietnam, Program with Abstracts, Hanoi, 23.

Flower, M.F.J., Tamaki, K., Hoang, N., 1998. Mantle extrusion: model for dispersed volcanism and DUPAL-like asthenosphere in east Asia and western Pacific. In: Flower, M.F.J., Chung, S.-L., Lo, C.H., Lee, T.-Y. (Eds.). Mantle Dynamics and Plate Interactions in East Asia. American Geophysical Union, Geodynamics Series 27, 67–88.

Flower, M.F.J., Chi, C.T., Yem, N.T., Mocanu, V.I., 2004. Editorial. Asthenosphere-lithosphere dynamic responses to Tethyan plate collisions (IGCP-430). Tectonophysics 393, 1–7.

Fontaine, H., Workman, D.R., 1997. Encyclopedia of European and Asian regional geology. In: Moores, E.M., Fairbridge, Rh.W. (Eds.), Encyclopedia of Earth Sciences Series. Chapman & Hall, London, pp. 774–782.

Hall, R., 2002. Cenozoic geological and plate tectonic evolution of SE Asia and the SW Pacific: computer-based reconstructions, model and animations. Journal of Asian Earth Sciences 20, 353–431.

Harland, W.B., Armstrong, R.L., Cox, A.V., Craig, L.E., Smith, A.G., Smith, D.G., 1989. A Geologic Time Scale 1989. Cambridge University Press, Cambridge, 263 p.

Harrison, T.M., Leloup, P.H., Ryerson, F.J., Tapponnier, P., Lacassin, R., Wenji, Ch., 1995. Diachronous initiation of transtension along the Ailao Shan—Red River shear zone, Yunnan and Vietnam. In: Yin, A., Harrison, T.M. (Eds.), The Tectonics of Asia. Cambridge University Press, New York, pp. 208–226.

Hawkesworth, C.J., van Calsteren, P.W.C., 1983. Radiogenic isotopes—some geological applications. In: Henderson, P. (Ed.), Rare Earth Elements. Elsevier, Amsterdam, pp. 375–421.

Hergt, J.M., Peate, D.W., Hawkesworth, C.J., 1991. The petrogenesis of Mesozoic Gondwana low-Ti flood basalts. Earth and Planetary Sciences Letters 105, 134–148.

Hoang, N., Flower, M., 1998. Petrogenesis of Cenozoic basalts from Vietnam: implication for origins of a 'diffuse igneous province'. Journal of Petrology 39, 369–395.

Hoang, N., Flower, M.F.J., Carlson, W.W., 1996a. Major, trace element, and isotopic compositions of Vietnamese basalts: interaction of hydrous EM-1—rich asthenosphere with thinned Eurasian lithosphere. Geochimica et Cosmochimica Acta 60, 4329–4351.

Hoang, N., Flower, M.F.J., Xuan, Ph.T., 1996b. Petrology of late Cenozoic basalts in Vietnam (in Vietnamese with English summ.). Geology and Natural Resources 1, 156–166 (Hanoi).

Hung, N.V., Vinh, H.Q., 2001. Moving characteristics of the Lai Chau-Dien Bien fault zone during Cenozoic. Journal of Geology, Series B 17/18, 65–77 (Hanoi).

Huppert, H.E., Sparks, R.S.J., 1985. Cooling and contamination of mafic and ultramafic magmas during ascent through the continental crust. Earth and Planetary Science Letters 74, 371–386.

Hutchison, C.S., 1975. Ophiolites in southeast Asia. Geological Society of America Bulletin 86, 797–806.

Hutchison, C.S., 1989. Geological Evolution of SE Asia. Oxford Monographs in Geology and Geophysics 13, 368.

Irvine, T.N., Baragar, W.R.A., 1971. A guide to the chemical classification of the common volcanic rocks. Canadian Journal of Earth Sciences 8, 523–548.

Ishii, T., 1975. The relations between temperature and composition of pigeonite in some lavas and their application to geothermometry. Mineralogical Journal 8, 48–57.

Jolivet, L., Beyssac, O., Goffé, B., Avigad, D., Lepvrier, C., Maluski, H., Thang, T.T., 2001. Oligo-Miocene midcrustal subhorizontal shear zone in Indochina. Tectonics 20, 46–57.

Kiem, D.D., Quy, H.H., Tuyet, D., Van, T.T., 1999. Some tectonic-structural characteristics of NW Vietnam. Journal of Geology, Series B 13/14, 96–106 (Hanoi).

Kitahara, S., Takenouchi, S., Kennedy, G.C., 1966. Phase relations in the system $MgO–SiO_2–H_2O$ at high temperatures and pressures. American Journal of Science 264, 223–233.

Kushiro, I., 1990. Partial melting of mantle wedge and evolution of island arc crust. Journal of Geophysical Research 95, 15929–15939.

Lacassin, R., Replumaz, A., Leloup, P.H., 1998. Hairpin river loops and slip-sense inversion on southeast Asian strike-slip faults. Geology 26, 703–706.

Lee, T.Y., Lo, C.H., Chung, S.L., Chen, C.Y., Wang, P.L., Liu, W.P., Hoang, N., Chi, C.T., Yem, N.T., 1998. $^{140}K/^{39}Ar$ dating result of Neogene basalts in Vietnam and its tectonic implication. In: Flower, M.F.J., Chung, S.-L., Lo, C.-H., Lee, T.-Y. (Eds.). Mantle Dynamics and Plate Interactions in East Asia. American Geophysical Union, Geodynamics Series 27, 317–330.

Leloup, P.H., Lacassin, R., Tapponnier, P., Schaerer, U., Dalai, Zh., Xiaohan, L., Liangshan, Zh., Shaocheng, J., Trinh, P.T., 1995. The Ailao Shan—Red River shear zone (Yunnan, China), Tertiary transform boundary of Indochina. Tectonophysics 251, 3–84.

Le Maitre, R.W., Bateman, T., Dudek, A., Keller, J., Lameyre Le Bas, M.J., Sabine, P.A., Schmid, R., Sorensen, H., Streckeisen, A., Wodley, A.R., Zanettin, B., 1989. A Classification of Igneous Rocks and Glossary of Terms. Blackwell Scientific Publications, Oxford, 193 p.

Le Pichon, X., Fournier, M., Jolivet, L., 1992. Kinematics, topography, shortening, and extrusion in the India–Eurasia collision. Tectonics 11, 1085–1098.

Lepvrier, C., Maluski, H., Tich, V.V., Leyreloup, A., Thi, Ph.T., Vuong, N.V., 2004. The early Triassic Indosinian orogeny in Vietnam (Truong Son Belt and Kontum Massif); implications for the geodynamic evolution of Indochina. Tectonophysics 393, 87–118.

Loubet, M., Sassi, R., DiDonato, G., 1988. Mantle heterogeneities: a combined isotope and trace element approach and evidence for recycled continental crust materials in some OIB sources. Earth and Planetary Science Letters 89, 299–315.

Maluski, H., Lepvrier, C., Jolivet, L., Carter, A., Roques, D., Beyssac, O., Tang, T.T., Thang, N.D., Avigad, D., 2001. Ar–Ar and fission-track ages in the Song Chay Massif: early Triassic and Cenozoic tectonics in northern Vietnam. Journal of Asian Earth Sciences 19, 233–248.

Maluski, H., Lepvrier, C., Leyreloup, A., Tich, V.V., Thi, Ph. T., 2002. Late Permian-Early Triassic thermotectonicsm in Vietnam (Truong Son Belt and Kon Tum Massif). Geodynamic implications. In: IGCP 430 Second Annual Workshop 'Mantle Responses to Tethyan Closure', April 1–10, 2002, Halong Bay City, Vietnam, Program with Abstracts. Hanoi, pp. 36–37.

McDonough, W.F., Sun, S.-S., Ringwood, A.E., Jagoutz, E., Hofmann, A.W., 1992. Potassium, rubidium and cesium in the Earth and Moon and the evolution of the mantle of the Earth. Geochimica et Cosmochimica Acta 56, 1001–1012.

Meschede, M., 1986. A method of discriminating between different types of mid-ocean ridge basalts and continental tholeiites with the Nb–Zr–Y diagram. Chemical Geology 56, 207–218.

My, B.P., Ky, P.V., Hoanh, N.V., Tuyet, T.D., 1978. Geological map of the Socialist Republic of Vietnam 1: 200,000, sheet Lao Cai (F-48-XIV). General Geological Directorate, Geological Survey Inter-Group, Hanoi.

Odin, G.S. (Ed.), 1982. Numerical Dating in Stratigraphy, vol. 2. Wiley-Interscience, Chichester, p. 1040.

Palmer, A.R., Geissman, J., 1999. Geologic time scale. Geological Society of America, Product Code CTS004.

Patchett, P.J., 1980. Thermal effects of basalt on continental crust and crustal contamination of magmas. Nature 283, 559–561.

Pearce, J.A., Cann, J.R., 1973. Tectonic setting of basic volcanic rocks determined using trace element analyses. Earth and Planetary Science Letters 19, 290–300.

Pécskay, Z., Balogh, K., Tóth, E., 2002. Radiometric age determinations of magmatic rocks from Vietnam. Institute of Nuclear Research, Hungarian Academy of Sciences, Debrecen, 9 ms. pp. (unpublished report).

Polyakov, G.V., Yem, N.T., Izokh, A.E., Balykin, P.A., Hoa, T.T., Phuong, N.T., Thanh, H.H., Hung, T.Q., 2002. Evolution of Mesozoic-Cenozoic mantle magmatism in the southern Indo-Sinian Mobile Belt (North Vietnam and Pamir-Himalayan folded systems). In: IGCP 430 Second Annual Workshop 'Mantle Responses to Tethyan Closure', April 1–10, 2002, Halong Bay City, Vietnam, Program with Abstracts. Hanoi, pp.45–46.

Rangin, C., Klein, M., Roques, D., Le Pichon, X., Trong, L.V., 1995. The Red River fault system in the Tonkin Gulf, Vietnam. Tectonophysics 243, 209–222.

Rollinson, H.R., 1993. Using Geochemical Data: Evaluation, Presentation, Interpretation. Longman Scientific and Technical/Wiley, New York, 352 p.

Saunders, A.D., Norry, M.J., Tarney, J., 1988. Origin of MORB and chemically depleted mantle reservoirs: trace element constraints. Journal of Petrology, 415–445 (Special Lithosphere Issue).

Schaerer, U., Zhang, L.-Sh., Tapponnier, P., 1994. Duration of strike-slip movements in large shear zones: the Red River belt, China. Earth and Planetary Science Letters 126, 379–397.

Son, Ph., 1978. Geological map of the Socialist Republic of Vietnam 1: 200,000, sheet Son La (F-48-XXVI). General Geological Directorate, Geological Survey Inter-Group, Hanoi.

Steiger, R.H., Jäger, E., 1977. Subcommission on geochronology: convention on the use of decay constants in geology and geochronology. Earth Planetary Sciences Letters 36, 359–362.

Tapponnier, P., Pelzer, G., Armijo, R., 1986. On the mechanics of the collision between India and Asia. In: Coward, M., Ries, A.C. (Eds.). Collision Tectonics. Geological Society Special Publication 19, 115–157.

Tapponnier, P., Lacassin, R., Leloup, P.H., Schaerer, U., Zhong, D., Haiwei, W., Liu, X., Ji, S., Zhang, L., Zhong, J., 1990. The Ailao Shan/Red River metamorphic belt: Tertiary left-lateral shear between Indochina and south China. Nature 343, 431–437.

Taylor, B., Hayes, D.E., 1983. Origin and history of the south China Sea basin. In: Hayes, D.E. (Ed.). The Tectonic and Geologic Evolution of Southeast Asian Seas and Islands, Part 2. American Geophysical Union Monographic Series 27, 23–57.

Thompson, R.N., 1984. Dispatches from the basalt front. 1. Experiments. Proceedings of the Geologists Association 95, 249–262.

Tri, T.V. et al., 1979. Geology of Vietnam (North part). Research Institute of Geology and Mineral Resources, Hanoi, 80 p.

Trinh, P.T., Lacassin, R., Tapponnier, P., Leloup, P.H., Yem, N.T., 1993. Evidence for active strike-slip movements in Northwestern Vietnam. Terra Abstracts, Supplement 1 to Terra Nova 5, 265.

Trinh, P.T. et al., 1999. Active tectonics and seismic hazard in Son la hydropower dam (North Vietnam). Journal of Geology, Series B 13/14, 19–32 (Hanoi).

Tung, N.X., Tri, T.V., 1992. Structural map of Vietnam 1: 1,000,000. Geological Survey of Vietnam, Hanoi.

Tuyet, T.D., Hoi, N.V., Hung, N.B., Thong, A.V., 1978. Geological map of the Socialist Republic of Vietnam 1: 200,000, sheet Dien Bien Phu (F-48-XX). General Geological Directorate, Geological Survey Inter-Group, Hanoi.

Wang, E., Burchfiel, B.C., Royden, L.H., Liangzhong, C., Jishen, C., Wenxin, L., Zhiliang, C., 1998a. Late Cenozoic Xianshuihe-Xiaojiang, Red River, and Dali fault systems of Southwestern Sichuan and Central Yunnan, China. Geological Society of America Special Paper 327, 108 p.

Wang, P.-L., Lo, Ch.-H., Lee, T.-Y., Chung, S.-L., Lan, Ch.-Y., Yem, N.T., 1998b. Thermochronological evidence for the movement of the Ailao Shan-Red River shear zone: a perspective from Vietnam. Geology 26, 887–890.

Watson, E.B., 1982. Basalt contamination by continental crust: some experiments and results. Contributions to Mineralogy and Petrology 80, 73–87.

Weaver, B.L., 1991. The origin of ocean island basalt end-member compositions: trace element and isotopic constraints. Earth and Planetary Sciences Letters 104, 381–397.

Wemmer, K., Sievers, H., Thang, T.T., Trinh, P.T., 1999. New hints for nappe tectonics in northern Vietnam by K/Ar dating of very low grade sediments. Journal of Geology, Series B 13/14, 107–109 (Hanoi).

Wilson, M., 1993. Igneous Petrogenesis. Chapman & Hall, London, 466 p.

Winchester, J.A., Floyd, P.A., 1977. Geochemical discrimination of different magma series and their differentiation products using immobile elements. Chemical Geology 20, 325–343.

Yem, N.T., Tri, T.V., Hoa, T.T., Thanh, H.H., Phuong, N. Th., Ha, L. Th. Ch., Anh, T.T., Anh, T.V., 2002. IGCP 43- 'Mantle Dynamics and Tethyan Natural Hazard Mitigation', Second Workshop, Field Trip Guide, April 1–10, 2002, Ha Long, Vietnam. Institute of Geological Sciences National Center of Natural Sciences and Technology, Hanoi, 18 p.

Zelazniewicz, A., Tran, H.T., Fanning, M., 2005. Continental extrusion along the Red River Shear zone, NW Vietnam: new structural and geochronological data. GeoLines 19, 121–122 (Prague).

Zhu, B.-Q., Wang, H.-F., Chen, Y.-W., Chang, X.-Y., Hu, Y.-G., Xie, J., 2004. Geochronological and geochemical constraint on the Cenozoic extension of Cathaysian lithosphere and tectonic evolution of the border sea basins in East Asia. Journal of Asian Earth Sciences 24, 163–175.

Zuchiewicz, W., Cuong, N.Q., 2002. Morphotectonic and seismic properties of the Dien Bien Phu fault in Vietnam. In: Program with Abstracts, IGCP 430 2nd Annual Meeting 'Mantle Responses to Tethyan Closure', April 1–10, 2002, Halong Bay City, Vietnam, pp. 84–85.

Zuchiewicz, W., Cuong, N.Q., Bluszcz, A., Michalik, A., 2004. Quaternary sediments in the Dien Bien Phu fault zone, NW Vietnam: a record of young tectonic processes in the light of OSL-SAR dating results. Geomorphology 60, 269–302.